DEUTSCHES ELEKTRONEN – SYNCHROTRON DESY

DESY 86-161
December 1986

HOW QUARKS CONVERT INTO JETS AND WHAT A JET REVEALS ABOUT QUARKS

A REVIEW OF e^+e^- JETS

by

P. Mättig

IPP Canada

and

Carleton University Ottawa, Ontario, Canada

ISSN 0418-9833

NOTKESTRASSE 85 · 2 HAMBURG 52

To be sure that your preprints are promptly included in the
HIGH ENERGY PHYSICS INDEX,
send them to the following address (if possible by air mail):

DESY
Bibliothek
Notkestrasse 85
2 Hamburg 52
Germany

DESY 86-161
December 1986

ISSN 0418-9833

How Quarks convert into Jets

and what a Jet reveals about Quarks

A Review of e^+e^- Jets

P. Mättig

IPP Canada
and
Carleton University Ottawa,
Ontario, Canada

Abstract

The measurements on properties of jets produced in e^+e^- collisions are reviewed. Special emphasis is given to the experimental information obtained on the space time development of jets and the evidence on coherent gluon emission. The recently published data on jets originating from a special kind of parton are summarised. How to extract the properties of the original parton from jets is discussed.

Talk given at the $XXVI^{th}$ Cracow School of Theoretical Physics in Zakopane June 1^{st} – 13^{th}, 1986

Contents

1. Introduction 1
1.1 Models 3

2. Experimental Insight into the Space-Time Development of Jets 5
2.1 Where is the Charge compensated ? 6
2.2 How does the total Energy influence Fragmentation 9
2.3 How are non - leading Quantum Numbers compensated ? 13
2.4 Conclusion 15

3. Special Problems in Quark Fragmentation 16
3.1 The String Effect 16
3.2 Coherent Gluon Emission 21
3.3 Baryon Production 26
3.4 Conclusion 31

4. Do Jet Properties depend on the primary Parton ? 32
4.1 Bottom Jets 33
4.2 Charm Jets 36
4.3 The light Quarks 36
4.4 Gluon Jets 40
4.5 Conclusions 43

5. From Jets to Partons 46
5.1 Measuring the Energy and Directions of the Partons 46
5.2 Measuring the Charge of the Partons 51
5.3 Measuring the Parton Flavour - c,b Tagging 52
5.4 Measuring the Parton Flavour - light Quark Tagging 54
5.5 The Measurement of Partons - Conclusions 55

6. Conclusions 56

Acknowledgements 57

References 58

1. Introduction

One of the major fields of research at the e^+e^--colliders PETRA and PEP has been the structure of jets. Besides the high partonic c.m. energy W accessible with these machines, e^+e^--annihilations offer some special advantages compared to lp (lepton -quark) or pp (- quark-quark) collisions.

1. The c.m. energy of the process is known to high precision and does not have to be inferred from the measurement of the final particles.

2. Jets from all flavours can be produced (at PETRA and PEP up to the bottom quark) in theoretically well understood ratios. This allows to study jets with a certain flavour and keep the background under control.

3. No other hadronic matter besides the parton jets spoils the complete measurement of a jet. E.g. also the low energy content of a jet can be studied.

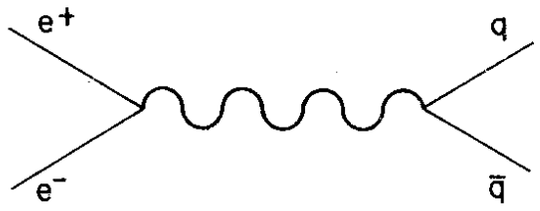

Hadron production in e^+e^--annihilation is considered to proceed via the production of a $q\bar{q}$-pair as shown in fig. 1.1. These quarks materialize into collimated bundles of particles : ' jets '. The properties of these jets reveal that they indeed originate from quarks.

1. The hadronic cross section in terms of the μ-pair cross section is ~ 4 [**1**] in rough agreement with the expectation from the quark-parton model

$$R = \frac{\sigma(e^+e^- \longrightarrow hadrons)}{\sigma(e^+e^- \longrightarrow \mu^+\mu^-)} = 3 \cdot \sum_{q=1}^{5} e_q^2 \sim 3.66$$

2. The angular distribution of the jets

$$1 + \cos^2\theta$$

[**2,3**] indicates that they stem from spin -$\frac{1}{2}$partons

3. The long-range charge correlations [**4**] (see section 2.1) give evidence that the first partons produced are charged.

4. The total charge within an event is not statistically distributed, but the average modulus of charge in a jet is 0.55 ± 0.25 [**5**] in agreement with what is expected for the mixture of quarks in e^+e^- annihilations.

It has been one of the prime discoveries at PETRA that at energies around 30 GeV about 10% of all events show a three jet structure. This can be naturally explained by hard gluon radiation.

- The events are planar [**6**] indicating that they arise from a three parton process
- The angular distribution of the jets indicates that this additional parton has spin 1 [**7**] .
- The $\sim$ 10% deviation of the total hadronic cross section from the quark-parton model can be explained by QCD-corrections and indicates an $\alpha_s \sim 0.1 - 0.25$ in rough agreement with the strong coupling constant obtained in deep inelastic scattering

These basic experimental evidences show a very good understanding of the general structures of hadronic events in e^+e^--annihilation in terms of hard partons and QCD. Still, the details of how these partons turn into the measurable hadrons are unsettled. An understanding of jet physics finally requires a theoretical description of the space-time development of jets.

There exists no detailed theoretical calculation of jet properties yet, but it is a general belief that it has to be related to non-perturbative QCD and the confinement of colour. Its energy scale is $O(1GeV)$, i.e. at low Q^2. The insight in jet development, however, has also substantial relevance in view of the new big machines starting to operate during the next years. Jets are the only information about quarks and gluons produced at these machines, and it is important in testing the standard model and searching for new phenomena within the energy regimes accessible with these colliders, to regard these jets as entities representing the fundamental hadronic partons. Discovering and analysing e.g. a new technicolor object requires the measurement of parton energies and directions as well as the determination of the parton kind. In how far the relevant informations can be extracted from the measurement of jets can be referred to as the 'high Q^2'-problem of jet physics .

In this report both questions will be covered. It starts with a discussion of what experimental information exists on how a jet develops. Special problems in fragmentation will then be addressed. The report continues summarising recent measurements on the fragmentation of known types of partons. It will end with a review of how well we will be able to determine the basic properties of the original partons.

2. Experimental Insights into the Space-Time Development of Jets

To obtain information on how the parton converts into hadrons, several experimental methods have been used. General constraints can be derived from the

- General topology of events (e.g. the limited transverse momentum with respect to the jet axis)
- Q^2-dependence of the jet properties (e.g. variation of transverse and longitudinal momentum with increasing c.m. energy W)

More details about the sequence of particle production within jets can be obtained by

- Studying quantum number compensation (e.g. examining if a charge within a jet is neutralised at random kinematical positions)
- Separating the hadrons containing the quark which is produced first (first rank hadron) and analysing the residual jet.

Results from these two methods will be discussed in this section. They allow one to achieve rather model independent insights into the space-time development of a jet. However, for a more quantitative and detailed understanding, kinematical effects like resonance decays, phase space etc. have to be separated and this requires a

- Comparison with models

The most popular models will be compared with measurements in section 3. Theoretically [**13**] a very interesting way to obtain information is to study

- The photon-bremsstrahlung off quarks. The key point in such an experiment is that since the photon can break through the gluon field without interactions it can reveal the state of the quark during the fragmentation process. However mainly due to the high background of photons from π^0-decays and initial bremsstrahlung, it is very difficult to discriminate direct photons from the final state. Up to now only the existence of quark-bremsstrahlung within a jet has been established [**14**] .

In the following some of the most important experimental results about the space - time development of a jet will be discussed

2.1 Where is the Charge compensated ?

In the Feynman-Field or LUND -scheme of fragmentation the produced meson picks up a certain fraction of the energy that is left over and statistically

$$y_1 \sim y_2 \sim y_3 \ldots\ldots$$

Here y_n is the rapidity

$$y_n = 0.5\, ln(\frac{E_n + p_{\parallel,n}}{E_n - p_{\parallel,n}})$$

of the n^{th} produced particle, E_n is its energy and $p_\parallel$ its momentum component along the jet axis. This leads to the expectation that quantum numbers are conserved locally, i.e. a meson with charge +1 is found in the vicinity of a meson with charge -1. In addition to this short range effect the leading particles of the two jets (at high $|y|$) are expected to contain the primary produced quark and thus to have opposite quantum numbers.

A schematic event built up according to these ideas is shown in fig. 2.1.1, where it is assumed that two particles with opposite charge are produced in each rapidity interval and only the leading particles are singly produced at high $|y|$. To analyse the charge correlation one defines a 'test charge' at y', sums over all possible combinations with other charged particles at any interval y and defines the charge-compensation asymmetry

$$A(y',y) = \frac{N^{+-,-+}(y',y) - N^{++,--}(y',y)}{N^{+-,-+}(y',y) + N^{++,--}(y',y)}.$$

In the case of the example this leads to an $A(y',y)$- distribution as shown in figs. d and e : defining the reference interval in the centre of an event, i.e. $y' \sim 0$ the short-range charge compensation induces a peak at $y \sim y'$. Defining the test interval to be at the position of the leading particle in one hemisphere, a peak at $y \sim -y'$ appears due to the emission of primary quarks.

Long-range charge correlations have been observed by four groups [**4,5,15,16**] . The CLEO - collaboration, although measuring at lower energies compared to the other experiments and thus being limited in the rapidity range, has the special advantage to be able to compare continuum events with data on the $\Upsilon(1S)$ which mostly decays into three gluons . Thus hadronic events originating from charged partons can be compared with those from neutral partons. Their results are displayed in fig. 2.1.2 .

Selecting the reference intervals in the rapidity range 0 to -2 the data in both cases indicate a short range compensation mechanism : the compensation function has rather high values. It is not obvious how to interprete these correlations. They can have either pure kinematic origin like coming from resonance decays (e.g. $\rho^0 \rightarrow \pi^+\pi^-$) or dynamic from the fragmentation process itself. Charge correlations are thus a complicated tool to study short range compensation. This problem will be rediscussed in section 2.3 .

1.1 Models

Basically there exist three kinds of QCD-motivated models for hadron production e^+e^- - annihilation.

- The Independent Jet model (e.g. of Field and Feynman [**8**]) iteratively combines the first produced quark q_1 with a quark-antiquark pair $q_2\bar{q}_2$ giving rise to a meson $(q_1\bar{q}_2)$ and the left over quark q_2 (fig. 1.2 a). The momentum of the meson is given according to an ad hoc probability distribution. The quark q_2 then undergoes the same procedure. This chain ends when all of the initial energy of q_1 is used up. The break-up of the initial quark into hadrons occurs independent of the initial antiquark which is treated in a similar but totally unrelated way as the quark. Only in the very last step the two jets from the quark and antiquark are merged to conserve energy, momentum and flavour. The model was extended to include hard QCD - effects by e.g. Hoyer et al. [**9**] .

- In the string model worked out in the LUND-simulation program [**10**] fragmentation occurs as a break-up of a colour neutral string formed between the quark and antiquark (fig. 1.2 b). Here the quark and the antiquark cannot fragment alone and confinement of colour is thus taken care of conceptually in the model (fig. 1.2 b). How the string breaks up , however, is not calculated from first principles but instead parametrised similar to the Independent Jet Model.

- The third class of models to describe fragmentation uses leading-log calculations in QCD and lets the initial off-shell produced quark cascade downwards in virtuality by gluon emission to some value of $Q^2 \sim (200\ MeV)^2$ [**11,12**] . This gluon distribution has then to be converted into a hadron distribution which is usually done by letting the gluons decay into a quark / antiquark pair and forming a colour neutral cluster. These clusters then decay into hadrons.

It should be noted that in all these models a considerable number of parameters is involved which cannot (yet) be calculated, but influence the predictions of the models considerably, both for the general features and in details. In addition it is sometimes uncertain how to parametrise the probability distributions to simulate the fragmentation process. Instead they have to be guessed. Thus to check the validity of a certain model requires a thorough evaluation of how far the results are based on some special parametrisation. The number of free parameters is especially high for the Independent Jet Model and the String Model, whereas the QCD-Shower Monte Carlos try to come along with rather few.

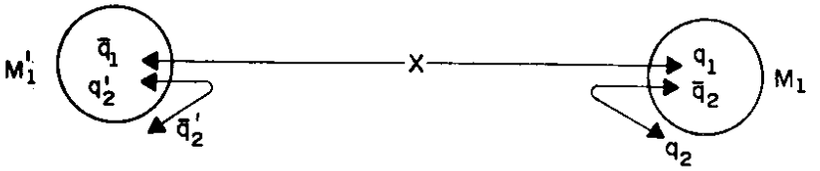

a.

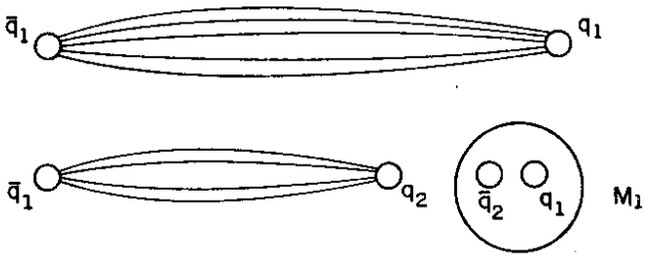

b.

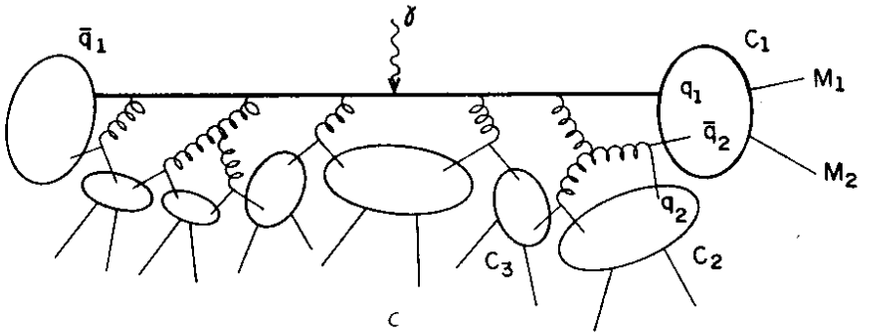

c

Increasing the rapidity values of the reference interval to y · 2 reveals a different behaviour in the two data samples. For the $\Upsilon(1S)$- data, i.e. the gluon jets, the charge of the reference particle is not compensated by particles with high rapidities in the opposite hemisphere ($y > 2$). However, for the continuum events, i.e. quark-jets, the compensation function shows a broad shoulder also at very high rapidity values.

This indicates that the primary partons produced in the e^+e^- -continuum are charged (one piece of the evidence for quarks mentioned in section 1.1) and the partons from the 1S-decay (gluons) are neutral. On top of that it also contributes essential information about the fragmentation process, showing that there exists a correlation between the rank of a hadron, i.e. at which stage in the sequence of fragmentation it is produced, and its value in rapidity. The fraction of particles containing the first produced quark is especially high in the high rapidity region. However, the compensation function has a value considerably smaller than one, the region in which the first hadron can be found is rather spread out.

2.2 How does the total Energy influence Fragmentation ?

In analogy to the scaling behaviour found in deep inelastic lepton-nucleon scattering a scaling behaviour in terms of

$$x_E = \frac{2 \cdot E}{\sqrt{s}} \sim \frac{2 \cdot p}{\sqrt{s}} = x_p$$

was also anticipated [**16**] within a quark-parton picture for fragmentation. x is the energy (or momentum) fraction of hadrons. Fig. 2.2.1 displays the scaled momentum distribution $\frac{1}{N_{ev}} \cdot \frac{dN}{dx_p}$ for c.m. energies between $\sqrt{s}$= 14 GeV and $\sqrt{s}$=34 GeV [**17**] . Neglecting the low x_p - region where mass effects are still important, the particle yield drops by only ~ 20% for $x_p > 0.2$, although the total energy is increased by about a factor of 2.5 . The small decrease of particle yield can be explained by QCD-effects [**18**] . In this context the focus of the discussion is on the approximate scaling behaviour. Within the models outlined in section 1.2 this feature is simulated by attributing the same scaled momentum probability distribution to the hadrons at each step in the chain of fragmentation. Within the QCD shower models the gluons emitted have (about) the same scaled energy spectrum. The scale is set by the energy of the quark which converts into the hadron, respectively the emitting quark or gluon. In such a way the parton 'forgets' the prehistory of the jet and initiates a chain of hadron production on its own.

A more direct evidence for such a behaviour has been published by the TASSO-collaboration [**19**] . They separated the first rank meson (a D^*) in charm events and compared the residual jets with an average jet produced at about the same residual energy. The procedure is sketched in fig. 2.2.2.

For the analysis the events with a tagged D^*were separated into two hemispheres with respect to the jet axis, the D^*- hemisphere and the unbiased charmed hemisphere

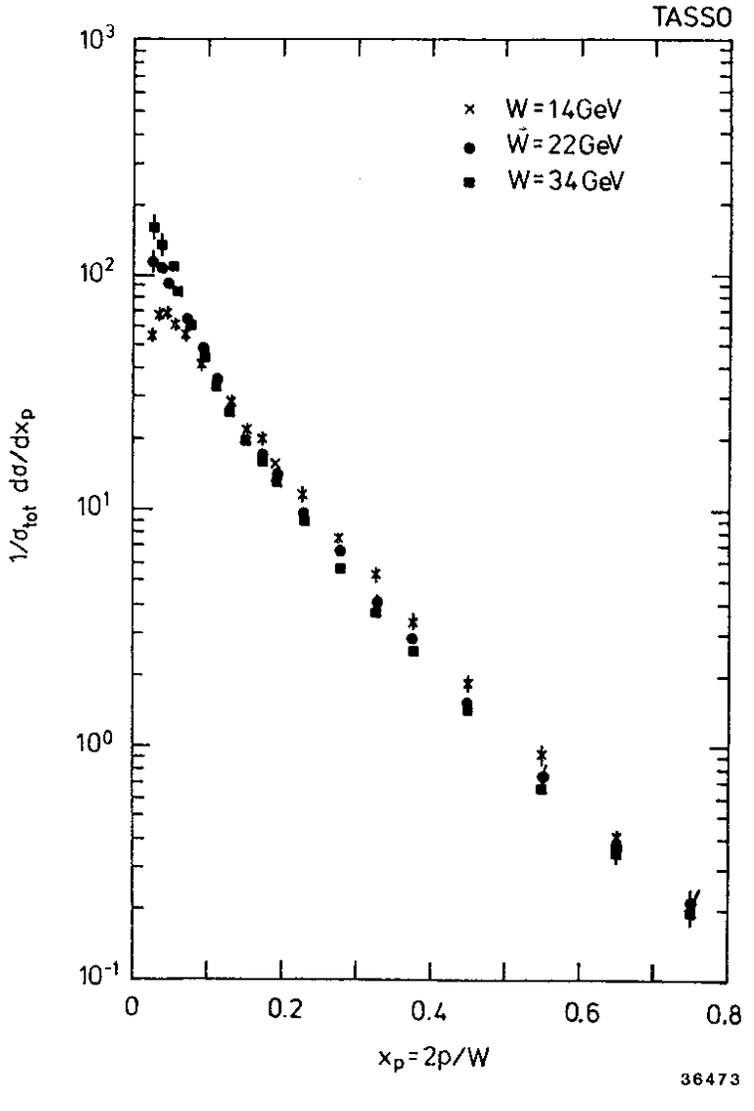

Fig. 2.2.1 Scaled momentum distribution $\frac{1}{\sigma_{tot}} \frac{d\sigma}{dx_p}$

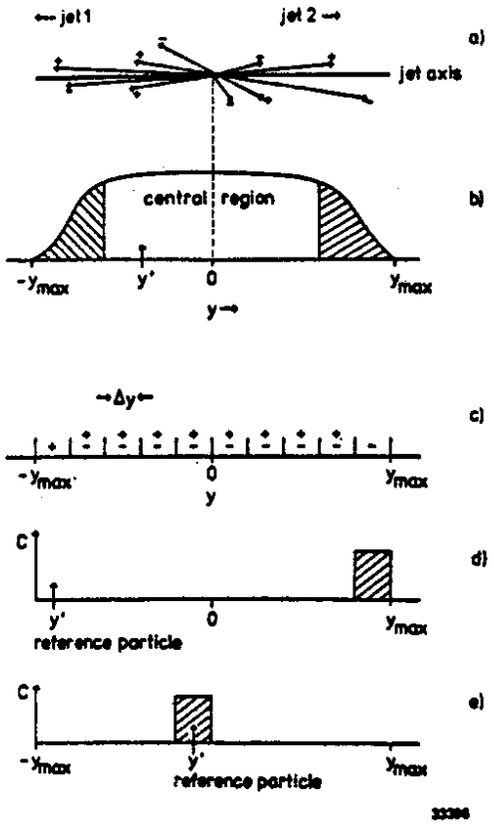

Fig. 2.1.1 Schematic event to interprete the charge compensation function

a. distribution of momentum vectors of charged particles

b. average rapidity distribution, shaded area indicates where the particle containing the primary quarks are expected.

c. charge distribution within intervals of size Δy.

d. charge compensation function for a reference particle at $y' = -y_{max}$

e. charge compensation function for a reference particle in the central region.

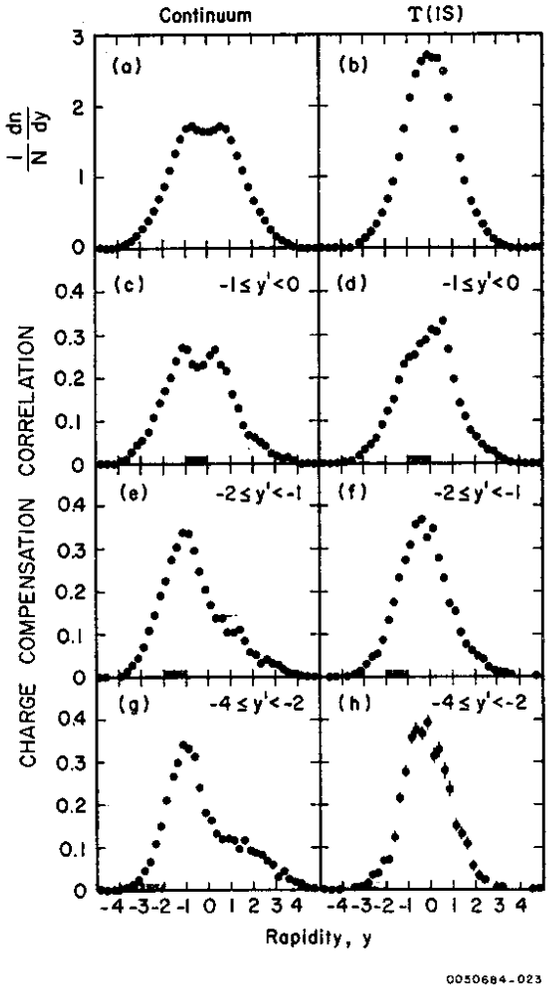

Fig. 2.1.2. Charge compensation function (a),(c),(e) and (g) in the continuum, i.e. $e^+e^- \longrightarrow q\bar{q}$; (b),(d),(f) and (h) on the $\Upsilon(1S)$- resonance,i.e. $e^+e^- \rightarrow ggg$. (a) and (b) display the rapidity distribution, the other histograms the charge compensation function for various reference intervals.

2.3 How are non-leading Quantum - Numbers compensated ?

In section 2.1 it has been shown that the rank (i.e. the place within the sequence of particle production) and the rapidity value of particles are correlated. The rapidity difference of two particles thus carries information about the relative ranks of particles, allowing one to study what kind of particles are produced in subsequent steps. In particular the rapidity difference of particles with compensating quantum numbers allows fundamental insights into jet development. As was discussed before, to be sensitive to the jet dynamics, effects originating from resonance decays have to be separated off. Thus the best probe are baryon-antibaryon pairs, which are unlikely to be remnants of heavier resonances. Results on $p\bar{p}$-correlations as well as on $\Lambda\bar{\Lambda}$-correlations have been published.

Background subtracted data	In same jet	In opposite jets
$e^+e^- \rightarrow p\bar{p}, p\bar{p} + X$	1.5 ± 2.1	3.5 ± 2.9
$e^+e^- \rightarrow p\bar{p} + X$	15.5 ± 4.5	1.2 ± 2.6

Table 1

Using their p and $\bar{p}$-identification over a large rapidity range the TASSO - collaboration studied how often $p\bar{p}$-pairs and $pp, \bar{p}\bar{p}$-pairs can be found in the same or in opposite jets [**20**] . The pp and $\bar{p}\bar{p}$ pairs presumably arise from the production of more than one baryon - antibaryon pair, where at least one of the partners evades detection. Such trivial correlations also exist for $p\bar{p}$ pairs and their rapidity differences should be alike. Thus pp and $\bar{p}\bar{p}$ pairs allow to reliably estimate the background for the true correlation studies. As can be seen from table 1 the baryon number is mostly compensated within a single jet, indicating short range compensation of the baryon quantum number. This result is supported by other TASSO-results examining protons with low rapidity values [**21**] .

The experimental results on the rapidity difference for $\Lambda\bar{\Lambda}$-pairs from two different experiments : TPC [**22**] , Mark II [**23**] are shown in fig. 2.3.1. TASSO [**24**] and CLEO [**16**] have obtained similar results.

Although the statistics is low (typically in 0.05% of all events a $\Lambda\bar{\Lambda}$-pair can be detected) the data show a preference for smaller differences in rapidity than expected from the single particle rapidity distribution folded and a rough agreement with the assumption of local baryon number compensation.

Each single piece of the data discussed exhibits only marginal significance, however, in combining the various experimental results on baryon - antibaryon number compensation, a consistent picture emerges : the baryon number is compensated in subsequent steps within the fragmentation scheme. To phrase it differently, the various steps are related by the emission of flavour neutral entities, which of course could be interpreted as gluons or clusters etc. in the various models discussed.

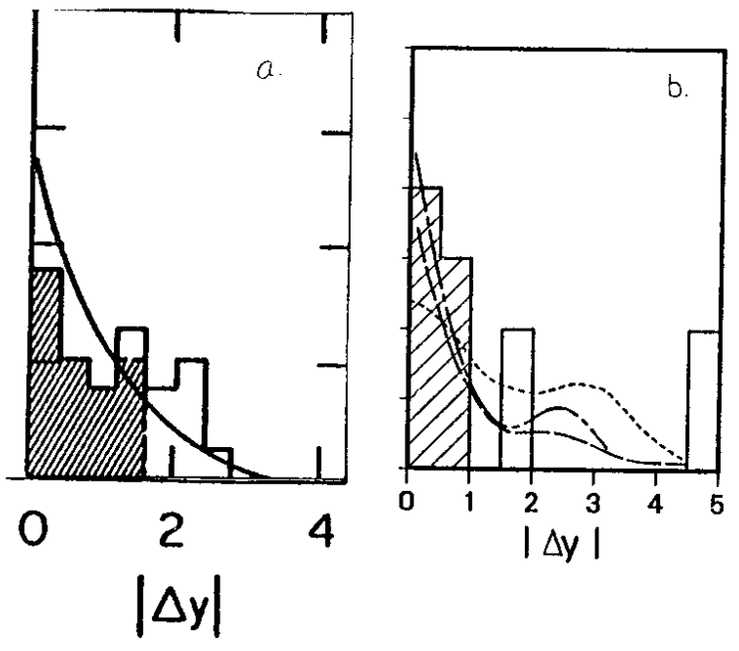

Fig. 2.3.1 Rapidity difference of $\Lambda\bar{\Lambda}$-pairs as measured by the Mark2 (a) and the TPC collaboration (b). The curve in a displays the prediction of a model that includes local quantum number compensation. The equivalent prediction in b is dashed-dotted, whereas the dotted curve is the expectation for an independent production of $\Lambda\bar{\Lambda}$-pairs.

Conclusion

The results presented so far, have all been derived without reference to a specific model, however they already constrain the phenomenology and models of jet development.

- The long range charge compensation suggests a correlation between the rank of a meson produced and its momentum. Especially the hadrons with the highest momentum (rapidity) tend to have the quantum numbers of the first produced quark.

- Fragmentation occurs stepwise and at each step the left over energy sets the scale for the fragmentation of the left over system.

- Short range baryon number compensation indicates that these steps occur by the creation of a flavour neutral entity (like a $q\bar{q}$-loop or a gluon). It then falls apart

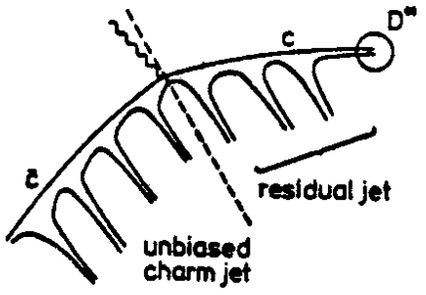

with respect to the jet axis. All particles in the D^*hemisphere with the exception of the D^*itself were considered as the 'residual jet'. The energy of this residual jet is

$$E_{RES} = W/2 - E_{D^*}$$

In the data-sample considered its average value is $< E_{RES} > = 6.2\ GeV$. To test the cascade-like mechanism the distributions of the residual jet were compared with the measured distributions of a jet produced at $E_{jet} = 17\ GeV$ and $E_{jet} = 7\ GeV$, an energy close to that of the average residual jet. The results are shown in fig. 2.2.3.

For all distributions $x_p = \frac{p}{E_{jet}}$, $x_r = \frac{p}{E_{RES}}$, rapidity y and p_T^2 with respect to the jet axis, the residual jet differs from the jet produced at 17 GeV. Partly this may be explained by phase space, however phase space should e.g. not influence the particle yield at low rapidities, but also here the residual jet differs from the 17 GeV-jet. In contrast to this, the jet produced with an energy of 7 GeV is in striking agreement with the residual jet. This strongly supports the idea of a cascade like fragmentation.

These results indicate that jet development proceeds via a series of discrete steps. However, it does not reveal how these steps look like. They are consistent with being formed by a quark picking up an antiquark from the 'sea' or a quark radiating a gluon, as implemented in the two basic approaches to jet formation discussed in 1.1. Each of the steps is rather independent of which particles and how they have been produced before. *

* This is obviously only shown within the statistical and systematic uncertainties of the data. Another theoretical point of view to be discussed in section 3.2 predicts that gluons are produced coherently effecting mostly the low energy particle distribution.

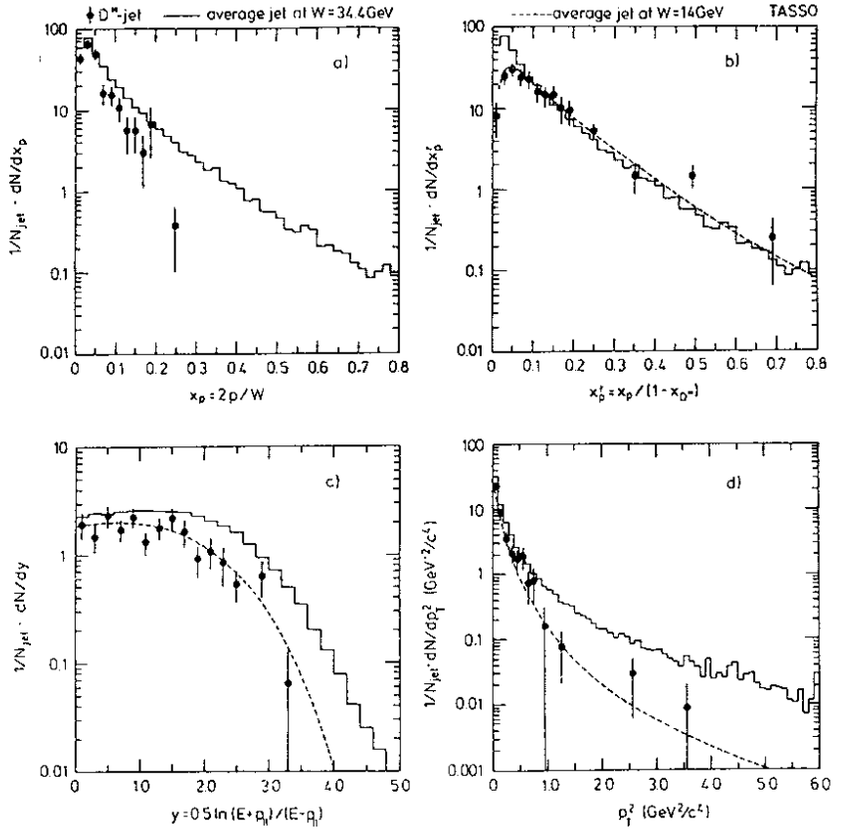

Fig. 2.2.3. Particle distribution in the residual jet (i.e. after separating the charmed particle from the hemisphere). Measurement : •, full curve : average jet W = 34 GeV, dashed curve : average jet at W = 14 GeV. a. scaled momentum distribution, b. scaled reduced momentum distribution, c. rapidity distribution, d. p_T^2 - distribution.

giving rise to a compensation of quantum numbers within a small energy-momentum (space-time) - interval.

These results are inconsistent with a purely randomised (longitudinal) phase space model, but they agree with other rather early developed ideas forming the basis of the Field-Feynman, the string or the QCD - shower approach. However these qualitative results do not discriminate between these models. To do this, the models have to be compared with the data in a more quantitive way.

3. Special Problems in Quark Fragmentation

3.1 The String Effect

Only one effect has been found so far enabling to discriminate between the models discussed in section 1.1, named 'string effect' which has been used to distinguish between the predictions of the Independent Jet Model and the LUND Model .

For $q\bar{q}$ events, i.e. without gluon radiation, no difference between the models can be found. In the Independent Jet Model two distinct systems $(q, \bar{q})$ fragment, while in the LUND Model only one system (the string between q and $\bar{q}$) fragments. However in both models, the fragmentation proceeds along the same axis in space (see fig. 3.1.1.a) and with appropriate, but possibly different parametrisations the same effective hadron distribution in the laboratory system can be accomplished.

This agreement ceases to be the case when hard gluons are emitted. In the Independent Jet Model fragmentation occurs in three systems (q, $\bar{q}$, g) whereas in the LUND Model it occurs in only two systems (the strings formed by q + part of the gluon and $\bar{q}$ + the other part of the gluon). The crucial point is that the fragmentation direction along the strings does not coincide with the parton directions (see fig. 3.1.1.b) as assumed in the Independent Jet Model .

This difference leads to different predictions for hadron distributions from these models for three jet events [**25**] and allows one to experimentally test the two approaches. In the string model it can be shown that for zero transverse momentum with respect to the fragmentation axis the produced particles lie along a hyperbola

$$\frac{p_x^2}{\beta^2\gamma^2 m^2} - \frac{p_y^2}{m^2} = 1$$

or

$$p_x^2 = \beta^2 \cdot \gamma^2 \cdot p_y^2 + \beta^2 \cdot \gamma^2 \cdot m^2$$

assuming the string moves in the x-direction with velocity $\beta = cos(\frac{1}{2}\theta_{qg})$ and γ the Lorentz boost of the string, where θ_{qg} is the angle between the quark and gluon. In the case of the Independent Jet Model ,however, the particles are distributed along the asymptotes of the hyperbola :

$$p_x = \pm\beta\gamma p_y$$

or

$$p_x^2 = \beta^2 \cdot \gamma^2 \cdot p_y^2$$

corresponding to the parton directions. This argument suggests that most of the difference between the two models should be found in the region between the parton directions and that especially particles with low momentum and high masses should reveal the difference.

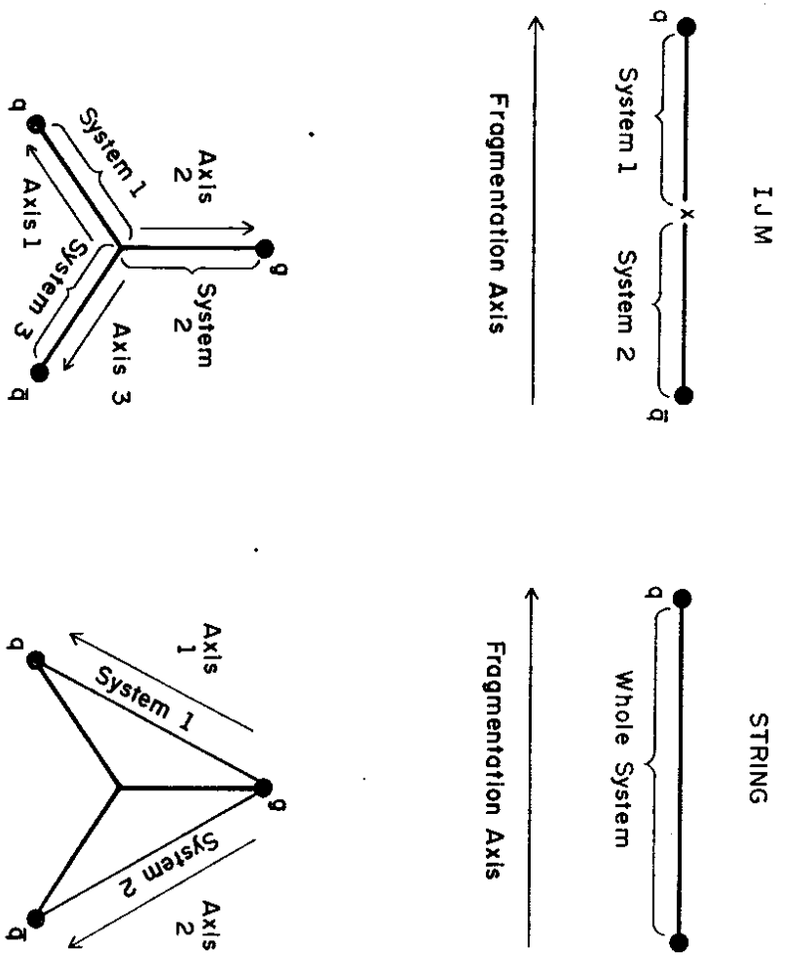

The JADE-collaboration [26] was the first to analyse their data searching for this effect. Only recently have their results been confirmed by the TPC [27] and the TASSO [28] collaborations. The basic steps in the analysis are

- select clear three jet events
- determine jet directions and energies
- sort jets according to their energy. Define the angles of the jets within the event plane to be $\theta_1 = 0$ for the most energetic jet, θ_2 for the second energetic jet and $\theta_3 > \theta_2$ for the least energetic jet. Statistically this means that jet 1 and jet 2 are mostly quark / antiquark jets whereas jet 3 mostly consists of the gluon jet.
- determine the angular flow of energy and particles in the event plane.

Fig. 3.1.2 shows the energy and particle flow as measured by JADE together with the predictions of the string (LUND) - model and the Independent Jet Model . As expected, the differences between the models show up in the region between the partons. The Independent Jet Model predicts a higher particle / energy yield in the region between jet 1 and jet 2 (i.e. between the quark and antiquark) however a lower yield between jets 2 and 3 as well as 1 and 3 (quark/ antiquark and gluon) compared to the LUND Model . The system of fragmentation in the LUND Model moves away from the region between the quark and the antiquark leading to a relative depletion there, but it moves into the region between the quark/antiquark and gluon , thus increasing the population of this region.

The data agree very nicely with the LUND-predictions but are inconsistent with the Independent Jet Model . As mentioned before , it is important to ensure, that this conclusion does not result from some inappropriate parametrisation but is inherent in the models. To this effect the TASSO-collaboration [28] has varied the parameters in the Hoyer et al. model quite considerably, especially the treatment of the gluon in that model: the momentum distributions of the quarks in the process $g \rightarrow q\bar{q}$ was varied, the quarks split off from the gluon obtained some relative p_T, the gluon fragmentation function was softened etc. However no way was found to match the distributions found in the data.

This is obviously a major success of the string model, which, as pointed out before, in addition has the stronger physics motivation than the Independent Jet Model . The string effect is important and significant, however it should be noted that only to a very small fraction of the tracks exhibit this different behaviour. Typically 10% of all events are selected as three jet events for such an analysis , the difference is significant only for a small fraction of the particles in these events, thus only about 0.5% of all particles exhibit the difference between the LUND Model and the Independent Jet Model .

For both models and especially the string approach it is rather striking, how well these relatively simple and ad-hoc ideas describe the data even up to the level of a parts per thousand.

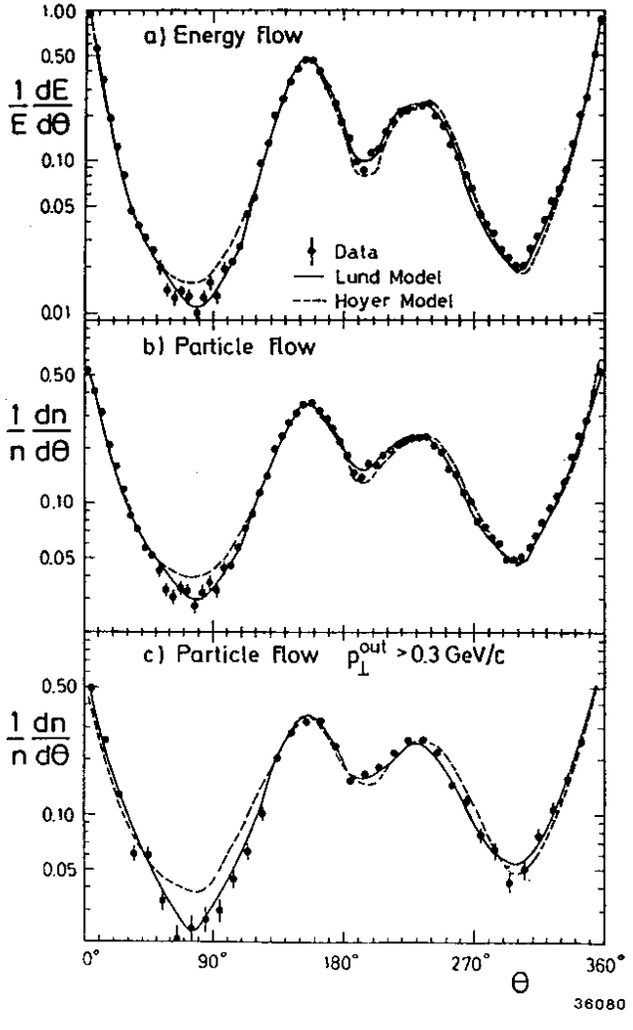

Fig. 3.1.2 Energy (a) and particle (b,c) flow within the eventplane. Measurements : • and model predictions from the string model (full line) and the Independent Jet Model (dashed line).

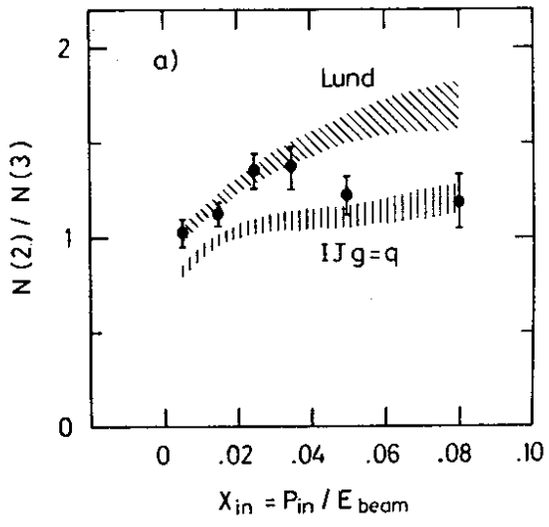

Fig. 3.1.3 Ratio of particle densities in the angular gaps between the jet axes as a function of $x_{in} = \frac{P_{in}}{E_{beam}}$ The model predictions are indicated by the shaded areas.

Just to indicate that also the LUND Model has its flaws, fig. 3.1.3 [**28**] displays the ratio of particle yield between jets 1 and 3 (N(2) ~ quark/gluon) over that between jets 1 and 2 (N(3) ~ quark/antiquark) depending on the scaled momentum of the particle in the event plane $x_{in} = \frac{P_{in}}{E_{beam}}$. Whereas at low x_{in}, for which the particle yield is largest, the data and the LUND-prediction coincide, they deviate for $x_{in} > 0.5$. In this region the Independent Jet Model shows a better agreement.

3.2 Coherent Gluon Emission

Major progress within the QCD - shower approach has been achieved during the last years. The basic step forward was the development of techniques to calculate the infrared logarithms up to leading order [**29,30**] in addition to the summation of the leading collinear logs exclusively used some years ago. The recent calculations show that interferences lead to the remarkable result that gluons are emitted coherently : the angle θ_n under which the gluon n is emitted depends on the angle θ_{n-1} of the gluon n-1 emitted earlier in the shower process .

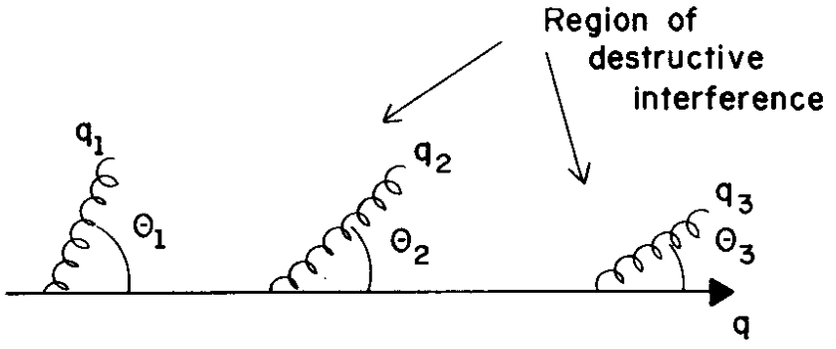

This is due to a negative interference in the region $\theta_{n-1} > \theta_n$ (fig. 3.2.1.) and leads to a dynamical reduction of phase space for soft gluons. Instead of a flat distribution in $\frac{d\sigma}{dln(\frac{1}{x})}$ the calculations predict for small x

$$\frac{d\sigma}{dln(\frac{1}{x})} \propto \exp\sqrt{\frac{2 \cdot c_A}{\pi \cdot b} ln(\frac{Q^2}{Q_0^2})} \cdot \frac{1}{\sqrt{ln^{\frac{3}{2}}(\frac{Q^2}{Q_0^2})}} \exp[-3\sqrt{\frac{8c_A}{\pi b}} \frac{(0.25 ln(\frac{Q^2}{Q_0^2}) - ln(\frac{1}{x}))^2}{ln^{\frac{3}{2}}(\frac{Q^2}{Q_0^2})}].$$

Here $c_A = 3$ and $b = \frac{33-2n_f}{12\pi}$ is related to the number of flavours n_f. Q_0 is the cutoff used which should be related to $\frac{\alpha_s(Q_0^2)}{\pi} \sim 1$, the limiting condition for a perturbative treatment of QCD. Using $\Lambda \sim 100\ MeV$ this translates into a $Q_0^2 = (200 MeV)^2$. The first exponential corresponds to the total multiplicity. As can be seen, a steep increase in the multiplicity with energy is predicted. The data are consistent with this prediction [**3**] . The second exponential describes the x-dependence of the particle yield and is seen to be

a Gaussian distribution with a central value of

$$ln(\frac{1}{x}) \quad 0.25 \cdot ln(\frac{Q^2}{Q_0^2})$$

A direct test of this prediction has been attempted by the TASSO -collaboration [**3**] and the by the HRS -collaboration [**31**] whose result is shown in fig. 3.2.2.

The distribution is consistent with the prediction showing a maximum at $x \sim 0.06$ or $Q_0 \sim 0.11$ GeV. A decrease in particle yield at low x-values is clearly visible. However, the calculations leading to the equation above, assumed massless partons and thus $x_p = \frac{2p}{W}$: $x_E = \frac{2E}{W}$. For the c.m. energies W, accessible at present e^+e^--colliders, the important region of the dip is at such low x-value, that $x_p \not\approx x_E$. The variable used in fig 3.2.2 is $x_p = \frac{2p}{\sqrt{s}}$. The measured distribution can be transformed if the particle content is known by

$$\frac{1}{\beta^2} x_p \frac{d\sigma}{dx_p} = x_E \frac{d\sigma}{dx_E}$$

Assuming that all particles at these low energies are pions (measurements indicate that this is true for $\sim 85\%$ of all the particles [**21,32**]) the dip is less pronounced as indicated by the dashed line in fig. 3.2.2. Even small amounts of heavier particles like kaons or protons would reduce the dip even more.

The TPC-collaboration [**32**] has published cross sections of identified particles up to very low x - values. Using these measurements to test the prediction in terms of x_E directly, reveals that only the pions show some depletion for low x_E, with a broad plateau around $x_E \sim 0.04$. No significant depletion can be seen for kaons and protons.

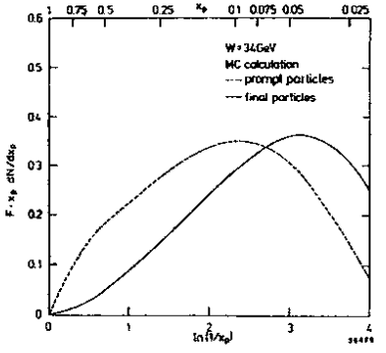

One of the difficulties to test the coherence prediction directly can be envisaged from fig. 3.2.3 . Here the results of a Monte-Carlo simulation (LUND-model) are displayed

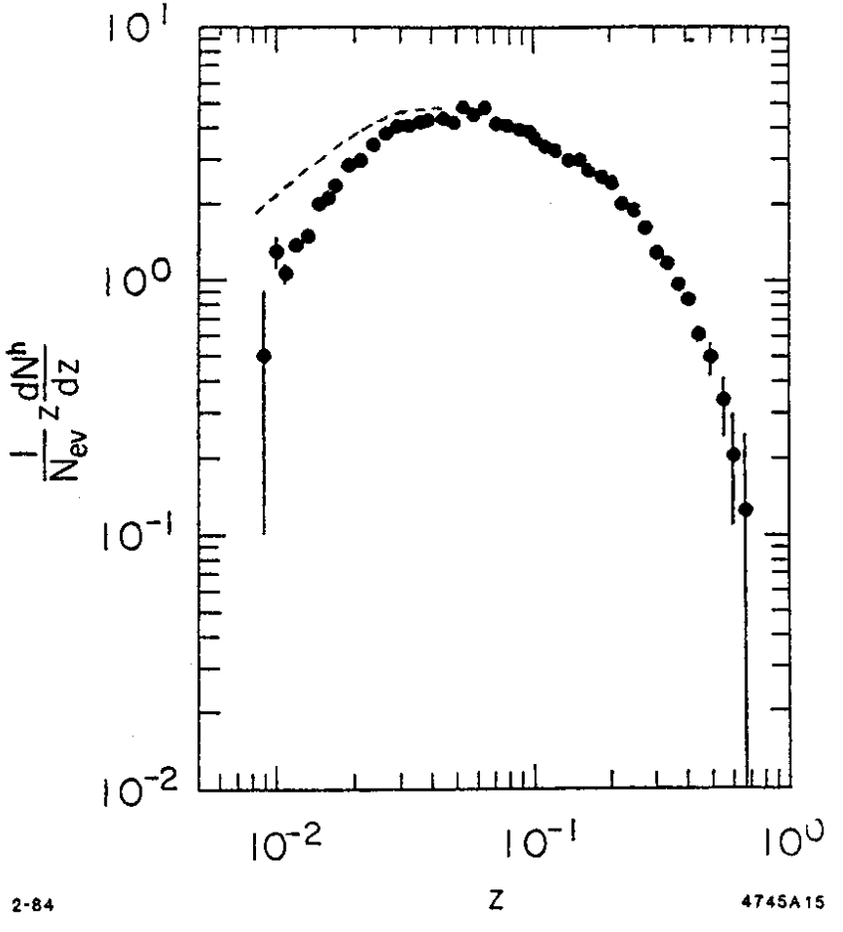

Fig. 3.2.2 Fragmentation function in terms of $\frac{1}{N_{ev}} \cdot z \cdot \frac{dN}{dz} = \frac{1}{N_{ev}} \cdot \frac{dN}{d \ln \frac{1}{z}}$, here $z = x_p$. The dashed curve indicates the result of a transformation $x_p \longrightarrow x_E$ assuming pion masses.

both for prompt and final (i.e. after decays) particle production. It indicates that decays considerably shift the position of the maximum and distort the distribution. The picture also indicates that the drop in particle yield is not a unique prediction of the leading log calculations, but is also inherent in classical approaches like the LUND Model .

From these arguments it seems to be difficult to test the coherence picture directly in the x-distribution . Consistency can only be expected if in addition to the dynamical properties of jet evolution the kinematical effects from particle decays are taken into account. Alternatively one can also assume a duality of the decay distribution of strongly decaying resonances and the dynamical properties of jet evolution ([**37**] ,see also [**33**]). The particle spectra from a mixture of these two sources are in this proposal not different to the outcome from jet evolution only.

The QCD matrix element including coherent gluon emission has been incorporated into the QCD- shower simulation by Marchesini and Webber [**11**] . As this matrix element only predicts the gluon distribution, they in addition had to adopt a phenomenological model to convert the gluons into hadrons. They followed the suggestion of Fox and Wolfram [**34**] who combined two partons to form colourless clusters of lowest possible mass, an idea closely connected to 'preconfinement' [**35**] . The clusters are considered to decay into pairs of hadrons according to phase space. Thus a comparison of this model with the data tests the mixture of the QCD matrix element and the cluster decay.

The application of the Webber model to the energy and particle flow in the event plane, the only distribution found so far that allowed to discriminate between models, revealed a surprising result [**36,27**] . This can be seen in fig. 3.2.4 where the data are compared with the Webber model and that of Gottschalk and Wolfram.

Both models are based on a QCD shower evolution, however only that of Webber and Marchesini has coherent gluon emission included. Not only the string model (as discussed in the previous section), but also the QCD shower model describes the data if and only if coherent gluon emission is included.

Since the Gottschalk-Wolfram model treats hadronisation the same way as the Webber model, this strongly indicates that the difference is indeed due to the interference terms. This is supported by fig. 3.2.5 where the parton flow as calculated in the Webber scheme is compared with that obtained by Gottschalk. As can be seen, the difference between the two approaches is already present on the parton level.

By studying the matrix element for the emission of a secondary gluon g_2 in $q_1\bar{q}_1g_1$ events, Azimov et al. [**37**] have shown, that up to $O(\frac{1}{N_c^2})$, where N_c is the number of colours, the angular distribution in $q\bar{q}g$ - events can be interpreted as an incoherent sum of two $q\bar{q}$ - systems. Due to the coherent emission of soft gluons there exists effectively a drag of low energy particles or g_2 by the gluon g_1. Note that the LUND Model treats the fragmentation just like this by splitting the gluon into a q_2 and a $\bar{q}_2$ which then form

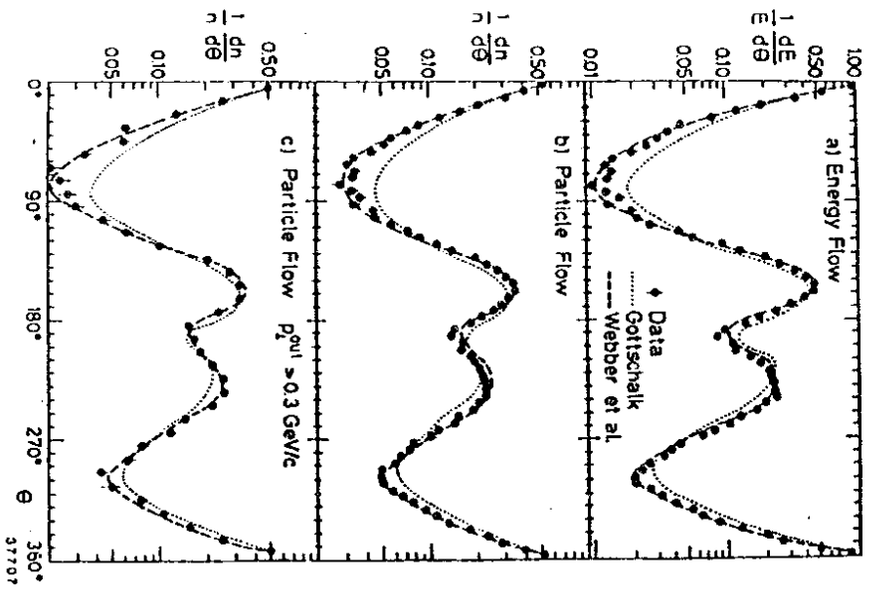

Fig. 3.2.4 Energy (a) and particle (b,c) flow within the event plane. Measurement and model predictions from the Webber model (full line) and the Gottschalk model (dashed line).

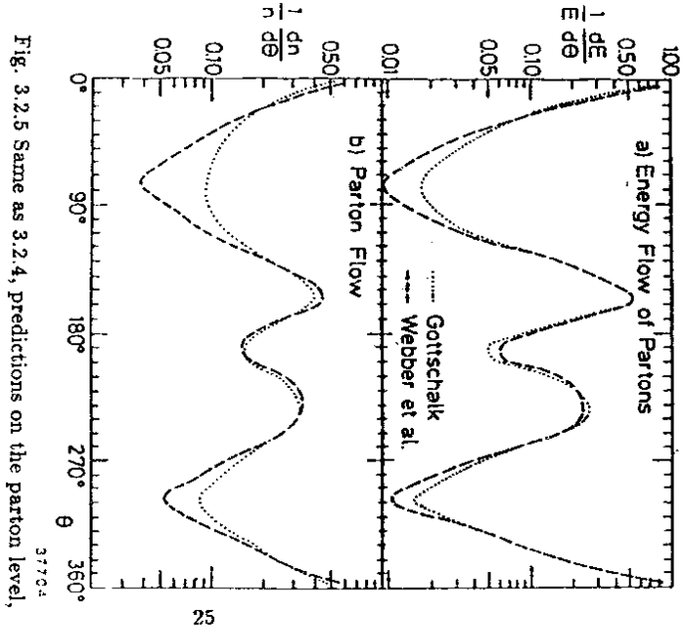

Fig. 3.2.5 Same as 3.2.4, predictions on the parton level, data points omitted.

number of s-quarks	name	yield/ev , W~ 30 GeV
Octet		
0	p	.64 ± .06
1	Λ	.23 ± .01
2	Ξ	.023 ± .008
Decuplet		
0	Δ	<0.09
1	$\Sigma^{*+/-}$	< 0.09
2	Ξ^{*0}	< /0.13
3	Ω	unclear

Table 2

separate strings of $q_1\bar{q}_2$ and $\bar{q}_1 q_2$.

To conclude this section : the feature typical for the classical string model can be described as well by a QCD leading log approach, if the coherent gluon emission leading to decreasing emission angles with decreasing gluon energy is included. To understand the close relation between the string picture and the QCD - shower approach will cast some light on the basic principles of jet development

3.3 Baryon Production

The first ideas on fragmentation assumed that only mesons are produced in a jet. However shortly after the turn-on of PETRA it was found that baryons are produced quite abundantly. Meanwhile several kinds of baryons have been found (or looked for without successs) with good enough precision to gain insight into how these baryons are produced.

Table 2 summarises the yields at $W \sim 30\ GeV$ [38] . Some regularities can be seen from this table :

- the baryon yield is roughly 8% of the meson yield
- strange baryons are suppressed
- decuplet baryons are produced much less often than octet baryons.

The ARGUS collaboration has used their high statistics and excellent detector performance for a systematic study of baryon production at $W \sim 10\ GeV$ [**39.**] They have established signals for most of the decuplet baryons and thus are able to determine production yields instead of upper limits. To reduce the systematic errors they quote production ratios instead of absolute yields.

- $\frac{\Xi^-}{\Lambda} = 0.08 \pm 0.01$
- $\frac{\Sigma^{*-}}{\Lambda} = 0.047 \pm 0.006^{+0.006}_{-0.005}$, $\frac{\Sigma^{*+}}{\Lambda} = 0.052 \pm 0.007^{+0.006}_{-0.004}$
- $\frac{\Omega^-}{\Lambda} = (5.4 \pm 1.8 \pm 1.2) \cdot 10^{-3}$
- $\frac{\Sigma^0}{\Lambda} = 0.33 \pm 0.11 \pm 0.09$
- $\frac{\Xi^{*0}(1530)}{\Xi^-} = 0.26 \pm 0.04^{+0.04}_{-0.02}$

The results are consistent with the limits obtained at higher energies [**40**] and quoted in table 2. They show also the regularities listed above.

The x-distribution of several kinds of baryons is shown in fig. 3.3.1 as measured by the TASSO-collaboration [**41**] . A comparison with the overall x - distribution (see fig. 2.2.1) suggests that the baryon fragmentation function is not very different to that of mesons. In particular, baryons are produced quite copiously also at high x-values.

The most popular models for baryon production can be classified into three kinds.

- A quark recombination model (e.g. [**42**]) assuming random occurence of a q,q,q -triplet in the $q\bar{q}$-sea. This idea has been already discussed in section 2.3 and has been shown to be incompatible with the short range correlation seen in the data.

- diquark models, where a diquark loop instead of a quark loop is inserted in the fragmentation chain (see fig 3.3.2) e.g. [**43,44**] . Such models predict short range baryon number compensation as seen in the data and naturally explain the regularities observed in table 2. Since strange diquarks are heavier than (u,d) - diquarks, and spin 1 - diquarks needed to form a decuplet baryon are heavier than spin 0 diquarks, both strange and decuplet baryons should be suppressed. On the other hand there exists no evidence for pointlike diquarks (e.g. from the total hadronic cross section in e^+e^- - annihilation) and thus it seems to be more appropriate to assume diquarks to be extended (e.g. [**45,46**]).

- Within the QCD-shower models baryons are produced in cluster decays. In the most easy version baryons are treated like mesons and only the cluster masses and the hadron masses determine their yield. As the masses of the clusters formed by gluons tend to be small $O(1-2\ GeV)$ and fall off rapidly , the low q-values in these

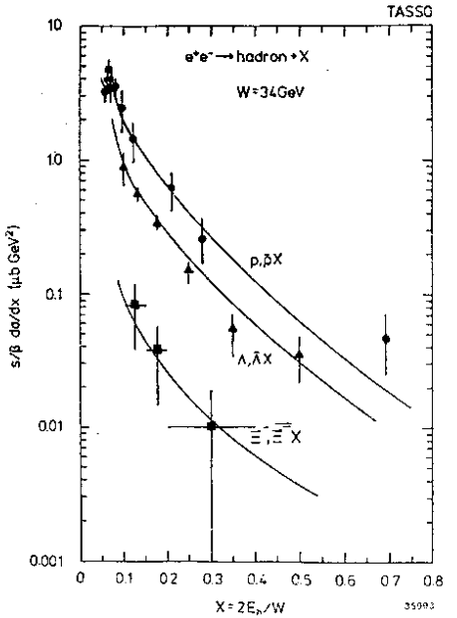

Fig. 3.3.1 Fragmentation function $\frac{s}{\beta} \cdot \frac{d\sigma}{dx_E}$ for different kinds of baryons : p,Λ,Ξ. Also shown are calculations with the LUND model.

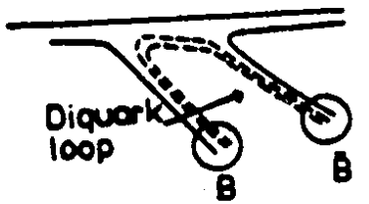

decays imply short range correlations. The overall rate can be made compatible with the measurement.

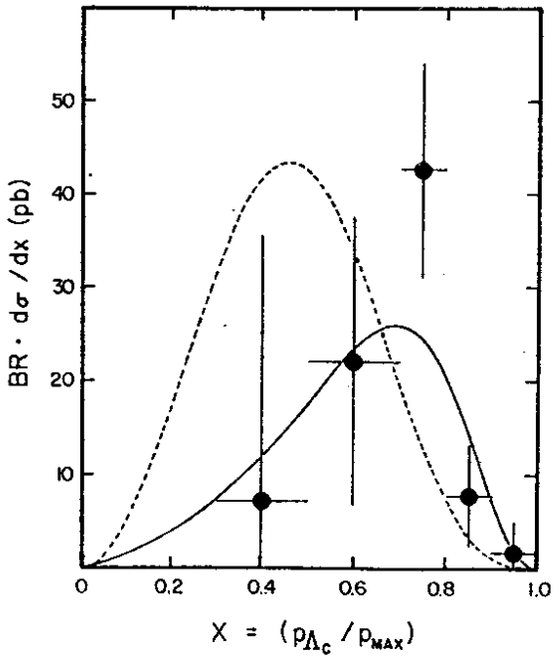

Fig. 3.3.3 Fragmentation function $BR \cdot \frac{d\sigma}{dx}$ for Λ_c production .Also shown are the theoretical predictions of Peterson et al. (full line) and de Grand (dashed line).

Already several arguments were given in favour of the diquark model. Fig. 3.3.3 shows another piece of evidence. The Λ_C-production measured by CLEO [**47**] is very well described by the standard charm fragmentation function [**48**] which assumes that a pointlike quark (or diquark) combines with a charm quark. Also shown is a prediction by de Grand [**46**] , who assumed a convolution of two single hard quark fragmentation functions (which corresponds to a specific form of an extended diquark) to combine with a charmed quark. As expected the extended diquark picture gives a softer fragmentation function than the pointlike. The data reveal that this specific model is wrong, however, they do not exclude other forms of extended diquarks.

Using the data on $p\bar{p}$-correlations the TPC-collaboration has compared the diquark model with the prediction from the cluster model [**11**] . They looked at the polar angle of the $p/\bar{p}$ in the $p\bar{p}$-rest frame with respect to the jet direction (determined with the sphericity tensor). Whereas the distribution from a cluster decay is flat due to the isotropic distribution generated in the model, the diquark model peaks as $\cos\theta^* = 1$ as expected from the limited p_T of hadrons with respect to the jet axis. These distributions are somewhat distorted by the experimental measurement. As can be seen from fig. 3.3.4 the data agree more with the diquark picture. Note however, that rather simple changes for

the cluster decay, can make the model agree with the data (see review on fragmentation models [**49**]).

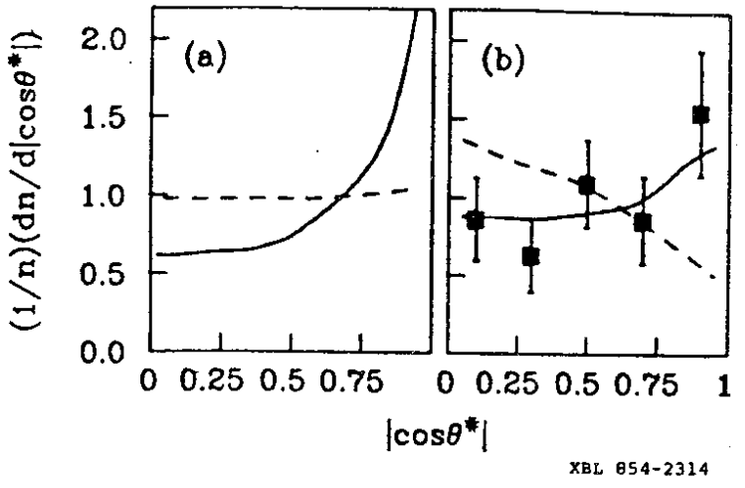

Fig. 3.3.4 Distribution of $p\bar{p}$-pairs in the angle θ^* between the proton direction and the sphericity axis, measured in the $p\bar{p}$-rest frame. Data and predictions of the LUND diquark model (full line) and the Webber cluster model (dashed line). (a) theoretical prediction assuming full acceptance, (b) experimental distribution.

3.4 Conclusion

Whereas generally the Independent Jet Model and the LUND Model can be tuned to describe the measurements of jet properties well, a more detailed comparison reveals important discrepancies. In particular the energy- and particle flow within three jet events is very well described by the string model, whereas the Independent Jet Model has inherent deficiencies. It seems remarkable that a classical model like that developed by the LUND-group is so highly consistent with the data.

Another class of models is based on QCD -shower calculations. These can only describe the data if coherent gluon emission is included. Without it, they disagree with the particle and energy flow in a similar way as the Independent Jet Model . It should be noted that the QCD - models are theoretically well founded only up to the gluon - distribution. Hadronisation has to be included phenomenoiogically. Discrepancies between data and the model can be cured by improving this part. The model, however, then looses some of its simplicity.

The relation between the string approach and the leading log calculations including interference is certainly one of the most interesting aspects in the understanding of jet development at the moment.

These models work to a high precision only if their parameters are fixed to special values. Conceptually these should be independent of the c.m. energy. However a comparison with data taken at different energies shows that this is not true. Especially for the LUND Model these parameters change from energy to energy indicating a rather fundamental problem. It is not only very inconvenient to fit these parameters again and again for different energies, but it suggests that the development of a jet is conceptually different from what the models suggest. Without an appropriate description of the c.m. energy dependence of jets there exists no real understanding of jets.

Baryon distributions are consistent with being produced by diquarks. However, no clear results about their pointlike nature have been obtained.

4. Do Jet Properties depend on the primary Parton ?

With the increasing understanding of the jet properties and the accumulation of hadronic events, it became possible to examine jets originating from a known type of parton. Such an analysis bears two important physics aspects. It contributes to the insight into the dynamics of jet development since it shows in how far jets are influenced by the first parton. In addition it points to the 'high Q^2-problem' addressed in the introduction : in the future one has to identify the original parton from the structure of a jet. As stated before, this has great relevance when examining the decay of massive objects into jets.

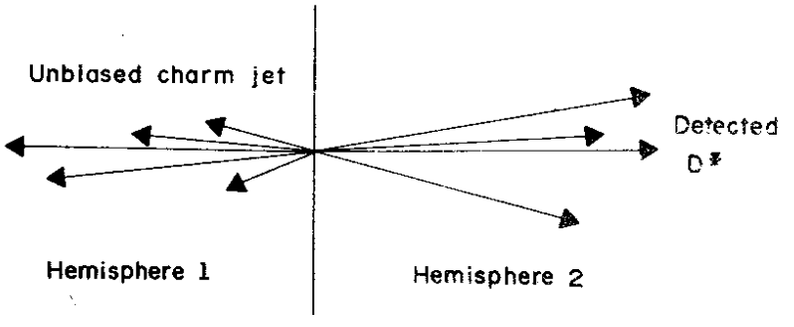

The basic method for this kind of analysis has been developed by the TASSO collaboration [19] and is sketched in fig 4.1. A hadronic event is divided into two hemispheres ('jets') with respect to the event axis. Only those events are considered, for which the original flavour in one jet can be determined by some special property such as an invariant mass reconstruction, the presence of high p_T-leptons etc.. Evidently the jet in which this feature is observed is biased. However, the jet in the opposite hemisphere is unbiased and known to have the same original flavour . This unbiased jet can be used to determine the general properties of jets with a special flavour.

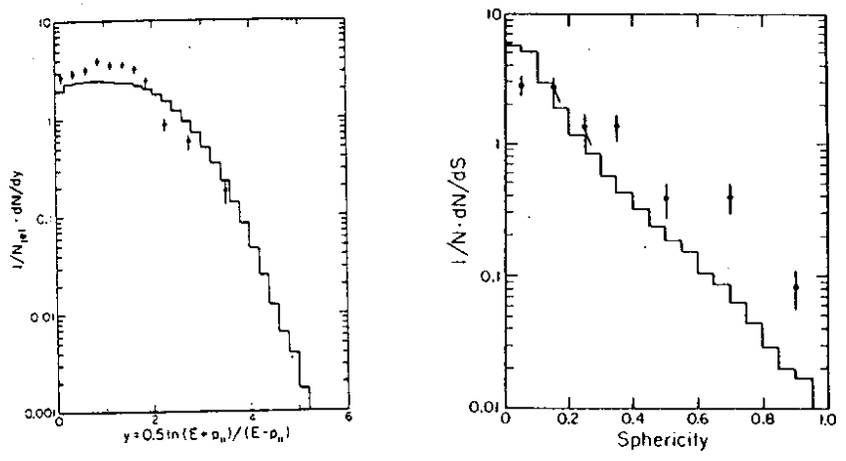

Fig. 4.1.1 Distribution of the rapidity (a) and sphericity (b) for unbiased bottom jets (•) and average jets (histograms).

4.1 Bottom Jets

The b-quark can be tagged by identifying high p_T-leptons. The detection of high p_T electrons down to rather low momentum has been used by the DELCO-collaboration [**50**] using data at W = 29 GeV to obtain a sample of 146 events, corresponding to about 2.4% of all b-events. The purity is high : $83 \pm 6\%$ of the events are coming from bottom quarks, $11 \pm 4\%$ from charm quarks and $6 \pm 2\%$ from u,d,s -quarks.

Fig. 4.1.1 shows their measurement of the rapidity and sphericity distributions of the unbiased jet. The measurement is compared with an average jet. Both distributions show distinct differences. The plateau in the rapidity is higher and shorter showing a bump

around $y \sim 1.5$. This distribution will be discussed in more detail below . The sphericity

$$S \quad \frac{3 \sum p_T^2}{2 \sum p^2}$$

is a measure of the broadness of a jet. S 0 corresponds to narrow jets, S 1 to a spherical event. As can be seen from fig. 4.1.2.b bottom jets at W 29 GeV are substantially broader than average jets.

Fig. 4.1.3 displays the rapidity distribution of b-jets in more detail. Also shown is the Monte-Carlo prediction (full line). As can be seen, the model describes the data very well. The simulation program allows to discriminate between particles originating from the first rank, i.e. the decay products of the bottom hadron, and those being produced in the subsequent fragmentation. From these curves it is seen that the hump-back at $y \sim 1.5$ mentioned above arises from the decay products of the b-hadrons.

This structure reflects the hard b-fragmentation function as well as the q-value of b-decays. The b fragmentation function at W $\sim$ 30 GeV has been measured to have an average value $< x > \sim 0.8$ (a recent compilation of measurements can be found in [**51**]) and a relatively small width $\delta x \sim 0.15$. As the b-hadron flies along the jet axis this can be related to rapidity values of $< y > \sim 1.4$ and $\delta y \sim 0.15$. In the b rest system the average rapidity $< |y| >$ of the decay products can be estimated by

$$< |y| > \sim 0.5 \cdot ln(\frac{< E > + < p_{||} >}{< E > - < p_{||} >})$$

Since the average charged decay multiplicity of B - mesons is $< n_{CH} > = 5.5$ [**52**] the average total multiplicity $< n >$ (before π^0 − decay) will be

$$< n > \sim \frac{3}{2} \cdot < n_{CH} > = \frac{3}{2} \cdot 5.5 = 8.3$$

and assuming

$$< p_{||} > = \sqrt{< p >^2 - < p_T >^2} \sim 0.62 \ < p >,$$

$$< E > = \frac{M}{< n >}$$

one obtains

$$< |y| > \sim 0.7 \Longrightarrow \delta(y_{decay}) \sim 0.9$$

for the b-decay products. Since the difference of the rapidities is Lorentz invariant under a boost along the direction of flight this leads to expect the b decay products to be centered around y $\sim$ 1.4 with a width of $\sigma(y) \sim 0.9$. This is in good agreement with the measurement from DELCO.

It is very tempting to exploit the different topology of b-jets compared to the average jets to select samples with an increased fraction of bottom events. This indeed has been done for lifetime studies, determination of the electroweak couplings of b-quarks etc.. For example in [**53**] the fraction of b-events has been increased from 11% to 33% with a $\sim$ 50% efficiency for b-events. These numbers, however, suffer from considerable systematic errors.

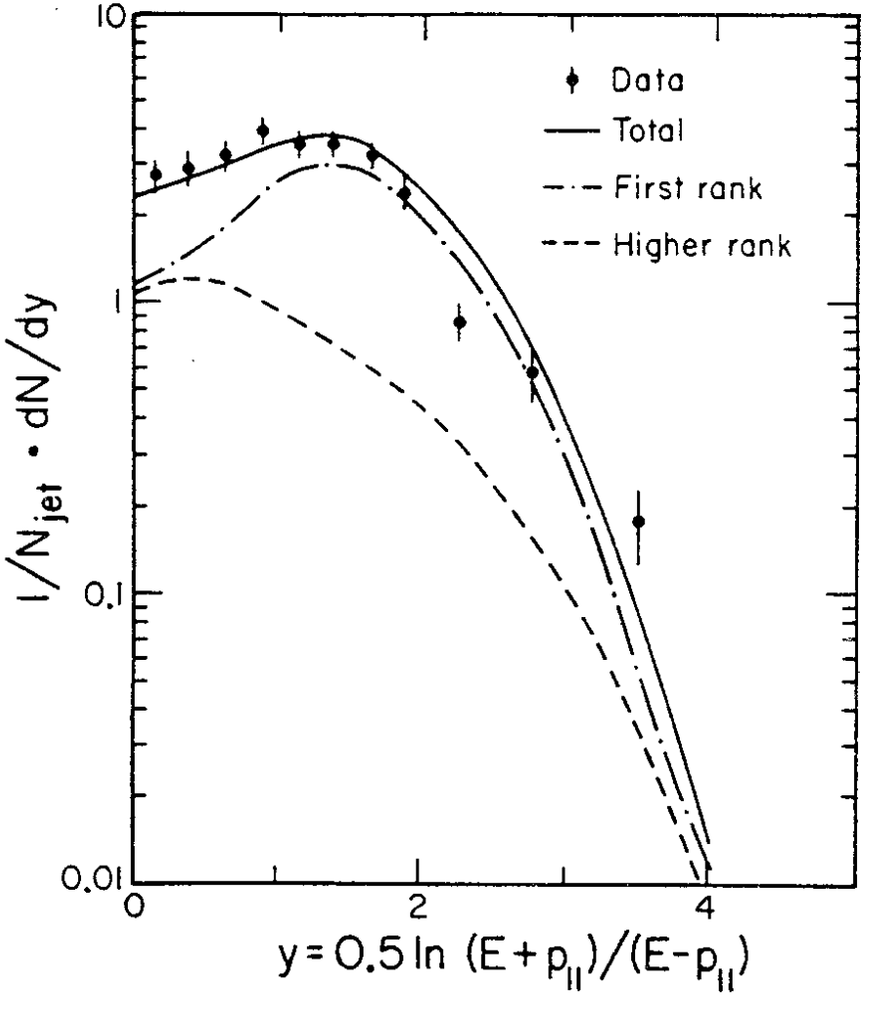

Fig. 4.1.2 Rapidity distribution of particles in an unbiased bottom jet. Data (•) together with model predictions : total particle yield (full line), decay products of B-hadrons (dashed dotted) and from the subsequent fragmentation (dashed).

4.2 Charm Jets

The first sample to study fragmentation properties of jets with a special flavour has been selected in the case of charm events by the TASSO - collaboration [**19**] . The sample was selected by reconstructing the D^*. It contained 82 events, corresponding to 1 % of all charm events, its purity was 80%.

Plotted in fig. 4.2.1 are the x-distribution, the rapidity, the p_T^2, sphericity and thrust distributions for the unbiased charm jet and the average jet. As can be seen, no obvious difference between the two samples can be observed. Note that the similarity of the distributions indicative of the width of the jets suggests that the QCD effects are similar in charm jets and in the average sample. A more detailed analysis to determine the α_s - value in charm jets can be found in [**54**] .

If we consider the hump-back seen in the bottom jets and repeate the argument given above, the charm decay products should be centered around $y \sim 2.3$. No such structure can be seen in fig. 4.2.1b. Since the charm fragmentation function is much wider ($\delta_y \sim 0.9$) than that of the bottom quark, decay products from charm particles in jets are expected to be found in a much broader rapidity interval and the hump back is smeared out in the charm case. In addition is the maximum in a region where the particle yield from the subsequent fragmentation is beginning to decrease. This decrease is partly compensated by the charm yield. The total result is that the rapidity plateau gets wider and no bump like that for bottom jets can be seen.

4.3 The light Quarks

No way has been found to tag u,d,s jets separately . The basic difficulty may be seen from the following example. Assume one can identify a strange particle containing the first quark, e.g. a K^+ . In contrast to charm and bottom discussed before, strangeness can also be picked out from the sea, so that a K^+ can be built out of a primary $\bar{s}$ quark combining with a u-quark or a primary u-quark catching a $\bar{s}$ quark from the sea. As determined from the relative yield of strange and non-strange mesons, about 44% of the quark-antiquark pairs in the sea are $u\bar{u}$-pairs, but only $\sim$ 12 % $s\bar{s}$. To estimate the reliability to identify strange jets through this mechanism, one has to compare the relative production of a K^+ from a primary $\bar{s}$-quark with that from a primary u-quark (negleeting c and b sources for a moment). The ratio of both alternatives is sketched in table 3 .

It can be seen that due to the small coupling of s-quarks to the photon and the production ratios of light quarks in the sea a K^+ from a primary s-quark is produced as frequent as from a primary u-quark. In addition, the soft fragmentation function of the light quarks and the abundant decays of the produced hadrons mixes the ranks even at high x-values. E.g. a K^+ from a second rank quark can have a larger x-values than the

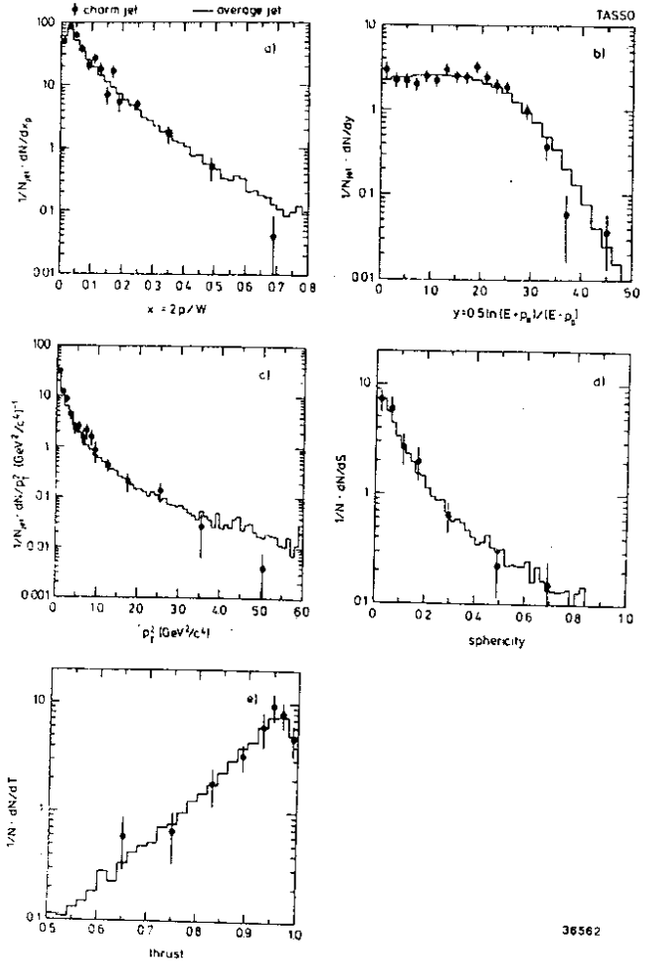

Fig. 4.2.1 Distributions for an unbiased charm jet (•) and an average jet (histogram) with $E_{jet} = 17\ GeV$

a scaled momentum distribution $\frac{1}{N_{jet}} \cdot \frac{dN}{dx_P}$

b rapidity distribution

c p_T^2-distribution

d sphericity and

e thrust

process	s-quark	u-quark
prim.	0.09	0.36
second.	0.44	0.12
total	0.04	0.044

Table 3

particle from the first rank . So at PETRA or PEP it seems difficult to tag u,d and s-jets separately. A calculation with the LUND Model for a c.m. energy of $W = 34\ GeV$ is displayed in fig. 4.3.1. Shown is the yield coming from a charged K originating from the first produced hadron in s-events. Also shown is the yield from other sources. Clearly the other sources contribute much stronger even at very high x-values and prohibit to tag strange flavour just by detecting a fast charged kaon.

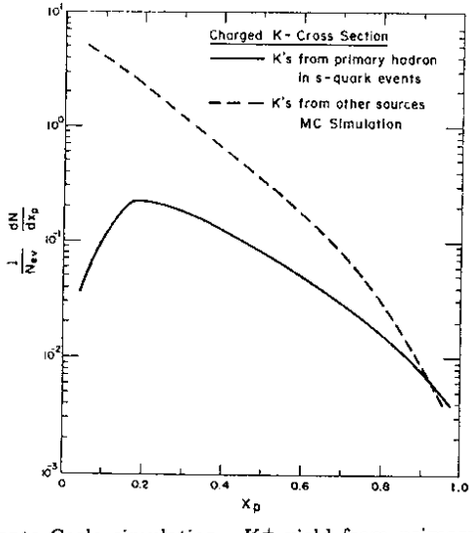

Fig. 4.3.1 Monte Carlo simulation. K^+-yield from primary s-quark and K^+-yield from other sources.

The HRS-collaboration [**55**] , taking advantage of their excellent momentum resolution, has tagged u,d and s-jets together by selecting events where at least one final particle

has a very high x-value. As the sample contains a mixture of primary flavours only limited conclusions can be drawn, e.g. little information about the electroweak couplings of light quarks can be obtained in that way. Fragmentation properties of light quarks can however well be studied.

At the first glance it seems to be surprising that one can obtain an u,d,s - sample by requiring a high momentum particle. The light quarks fragment soft, while the heavy quarks have a hard fragmentation function. However, the measurement is restricted to stable particles and the corresponding descendants are found at different x-values. All c and b hadrons decay with a quite high average decay multiplicity and their remnants have substantially lower x-values than their parent particles. On the other hand only approximately half of the hadrons from the light quarks decay, and if they do their decay multiplicity is rather small. The sum of all these effects is that the fraction of u,d,s remnants at high x is large.

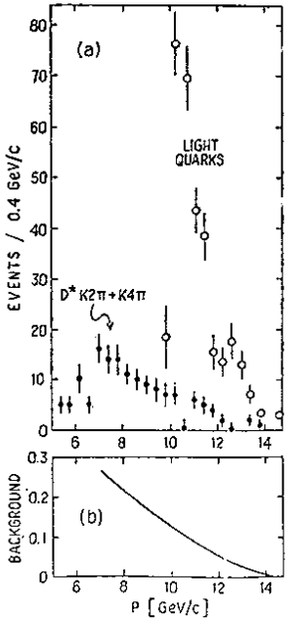

Fig. 4.3.2

a. Momentum spectrum of trigger particle for light quark selection. In addition the momentum spectrum of D^* is shown.

b. Monte-Carlo prediction of charmed and bottom quark contamination in the light quark sample as a function of the cut-off momentum.

The results of the HRS - collaboration are displayed in fig. 4.3.2 . In fig. a the spectrum of the measured trigger particle is shown together with the spectrum of reconstructed D^*s. A charged trigger particle is defined to have a scaled momentum $x_p > 0.7$. The fraction of charm and bottom events in the event sample selected by demanding a particle with momentum $p > p_{cut}$ can be read off from fig b. As can be seen choosing $p_{cut} = 10.15$ Gev/c, as applied by the HRS collaboration, allows a high purity u,d,s-sample to be selected, leaving a fraction of about 11% of c and b -events in the sample.

By this method 314 events out of a total of $\sim$ 40000 are retained corresponding to an efficiency for u,d,s - tagging of 1.4 % .

Using this event sample a cleaner comparison of charm jets with u,d,s jets can be achieved, without refering to an average jet sample (which contains about 36% charm events). However, as can be seen in fig. 4.3.3 the particle distribution measured in the two event samples of uds-jets (a) and charm jets (b) are very similar and thus the conclusions of the TASSO - collaboration are essentially confirmed by these data. A small difference is found in the average multiplicity (see table 4).

4.4 Gluon Jets

The analysis of properties of the gluon jets at PETRA and PEP is complicated by the problem of how to determine the energies of the jets and what particles to associate to a certain jet. First results on the p_T distribution in gluon jets have been published in [**26**] , and on the particle content in gluon jets e.g. in [**24**] and [**56**] . The Mark II [**57**] and the HRS -collaboration [**58**] have used the large number of events collected at PEP to overcome that problem by selecting rather rare symmetric 3-jet events, i.e. events where all jets have an angle of 120 degrees with each other. For those events the jet energy is known to be $E_{jet} = W/3$ and the background from events not containing gluons is negligible.

To obtain the x-distribution of gluon jets, the Mark II - collaboration first determined the average fragmentation function in the three jets in terms of $x = \frac{p_{had}}{E_{jet}} = \frac{3 \cdot p_{had}}{W}$. This distribution is a mixture of the gluon jet and two quark jets. To isolate the fragmentation function of the gluon jet, the x-distribution obtained from events at $W = 2 \cdot E_{jet}$, which contain nearly exclusively quark jets, is subtracted.

The results of the average jet at W = 29 GeV together with the unfolded gluon fragmentation function and the x-distribution of quark jets at $W = \frac{2}{3} \cdot 29 = 19.4\ [GeV]$ is shown in fig. 4.4.1 . The particle yield at lower x is higher in gluon jets than in quark jets, an opposite behaviour can be seen at higher x-values, suggesting a softer gluon fragmentation function.

This has been expected theoretically and is qualitatively in agreement with recent results from the $Sp\bar{p}S$ - collider [**59**] . To compare the measurement with model calcu-

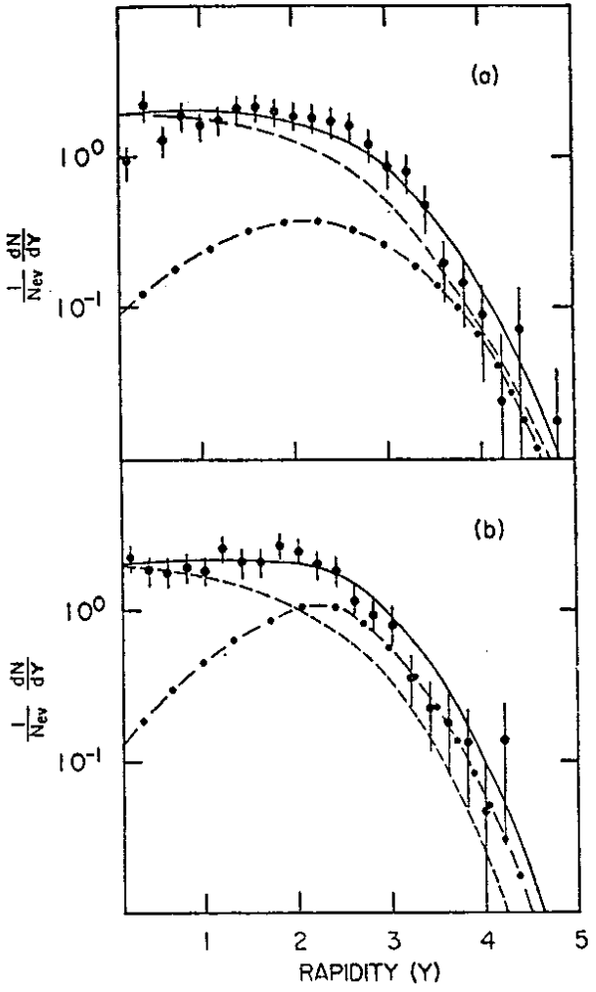

Fig. 4.3.3 Rapidity distribution for particles in (a) uds events and (b) c-events. The lines correspond to Monte-Carlo simulations : full lines = total particle yield, dashed-dotted lines = distributions of the decay products of the primary hadrons and dashed lines = hadrons from the sea quarks.

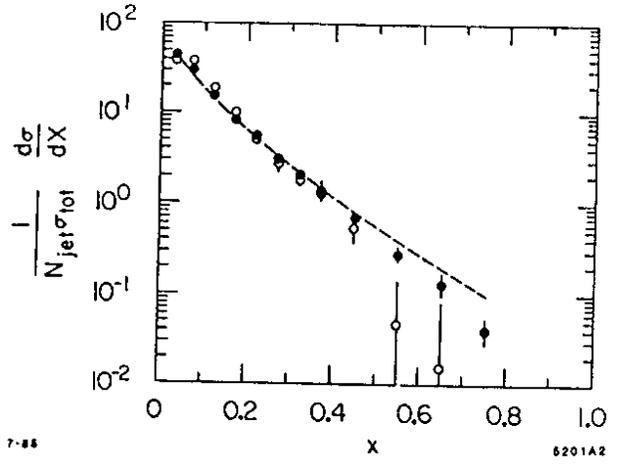

Fig. 4.4.1 Charged particle distributions $\frac{1}{N_{jet}} \cdot \frac{1}{\sigma_{tot}} \cdot \frac{d\sigma}{dx_p}$.Measured distribution (full symbols), interpolated distribution at $\frac{2}{3} \cdot E_{cm} = 19.3\ GeV$ and unfolded distribution of the gluon (open symbols).

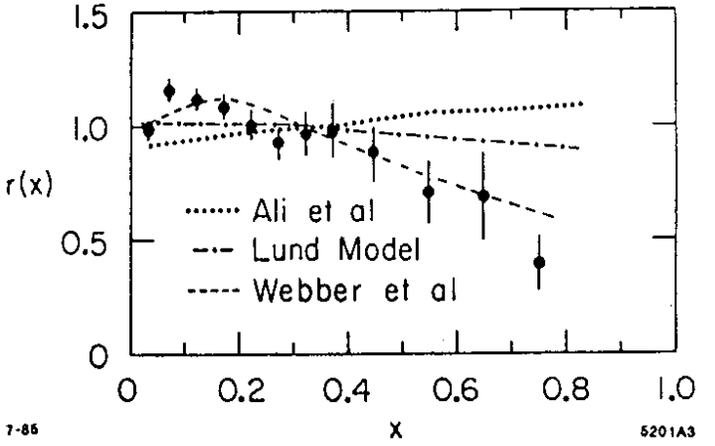

Fig. 4.4.2 Ratio of inclusive charged particle distribution for 3-fold symmetric 3-jet events at $E_{cm} = 29\ GeV$ to the inclusive charged particle cross section for hadronic events at $E_{cm} = 19.3\ GeV$ together with several model predictions.

lations, the MarkII - collaboration has calculated the ratio of the particle yield in three jets over that observed in two jets at the same jet energy and compared the ratio with the prediction from the Independent Jet Model [**60**] , the LUND Model [**9**] and the QCD Shower Model [**11**] . As can be seen from fig. 4.4.2 the data agree nicely with the QCD Shower Model , whereas both Lund and the Independent Jet Model predict the gluon to fragment too hard.

4.5 Conclusions

The measured multiplicities within jets of tagged partons for a jet energy $E_{jet} \sim 15\ GeV$ is listed in table 4. The differences observed are of the order $\sim 20 - 25\%$ between the different flavours. The ratio of the multiplicities in gluon and quark - jets is smaller than the theoretical prediction [**e.g.62**]

$$\frac{< n >_g}{< n >_q} = \frac{9}{4} - (QCD - corrections)$$

where the QCD - corrections are of the order 10%. It agrees with the LUND - prediction. The discrepancy with the QCD calculation is probably due to the limited phase space at present jet energies.

To summarise, very small differences between u,d,s,c and gluon jets have been found, only jets originating from the b-quark exhibit special properties. These results support the result from the TASSO-collaboration already discussed in section 1.2 that the jet develops independently of the flavour of the first quark (neglecting phase space effects due to the different masses of the corresponding hadrons). In this view topological flavour tagging seems to be difficult and may only be possible for b-jets at PETRA an PEP -energies. Other criteria like high p_T-leptons etc. seem to be more powerful for flavour tagging.

parton	$< n_{CH} >$	comment
uds	5.9 ±0.1 [**59**]	
c	6.6 ±0.15 [**59**]	c decay ~2.3 [**61**]
b	7.9 ±0.40 [**51**]	b decay ~5.6 [**53**]
gluon	$1.25^{+0.15}_{-0.15} < n_q >$ [**58**]	E_{jet} = 9.4 GeV

Table 4

We close this chapter by showing the substantially different event topology to be expected, if a new quark exists and the c.m. energy is close above the threshold. The

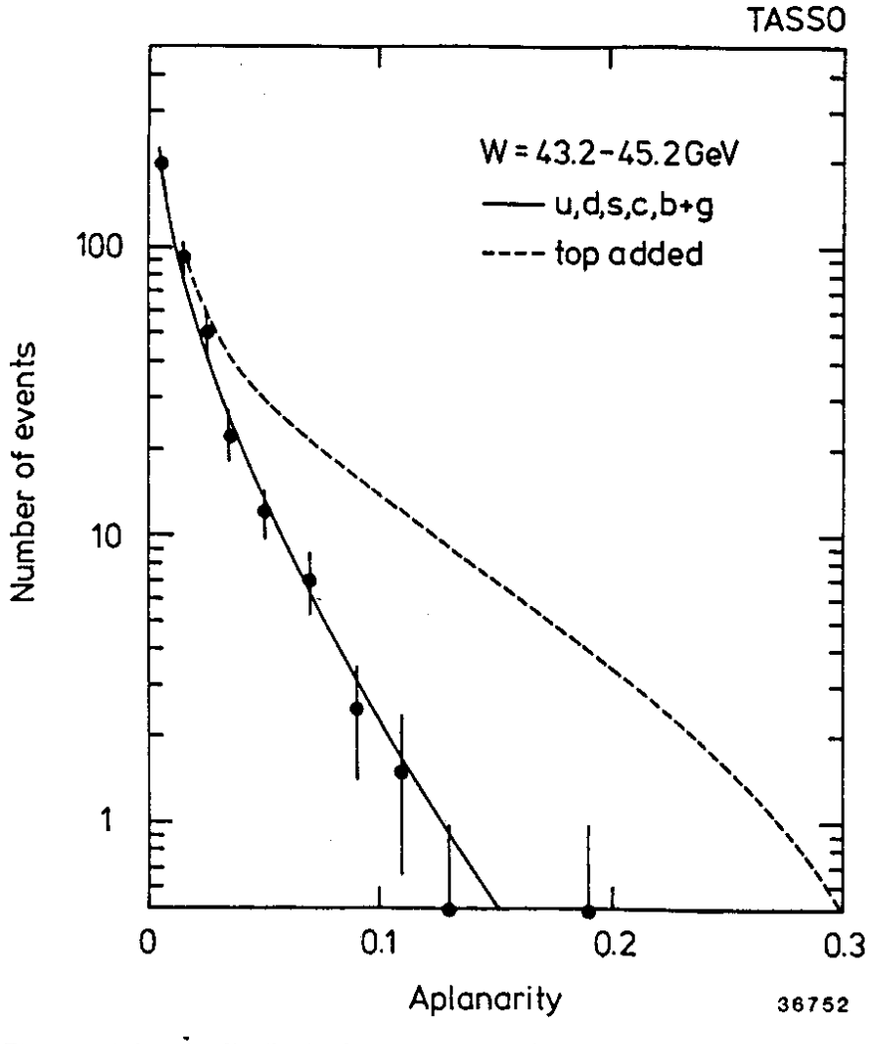

Fig. 4.5.1 Aplanarity distribution for events measured at $43.2 < W < 45.2\ GeV$. Also shown are model predictions for u,d,s,c,b+gluon events and with an additional top quark assuming $M_t = 20\ GeV$

distribution in the aplanarity A of an event

$$A = \frac{3}{2} \frac{\sum p_{Tout}^2}{\sum p^2}$$

where p_{Tout} is the momentum component out of the event plane, is shown in fig. 4.5.1 [**63**] . The distribution measured for 43.2 $\leq W \leq$ 45.2 GeV is compared with the model prediction for five quarks and QCD-bremsstrahlung as well as for an additional top-quark with a mass $m_T = 20\ GeV$. The top quark leads to a considerably wider distribution in the aplanarity. At PETRA-energies this distribution was used to set limits on the mass of a top-quark. For future colliders, however, this distribution may be used to select a clean sample of top - events.

5. From Jets to Partons

The High Energy Physics community is facing a new generation of accelerators with energies reaching beyond the standard model. The intermediate vector bosons and possible new high mass objects decaying into quarks and gluons will be produced, e.g.

- $e^+e^- \rightarrow W^+W^- \rightarrow hadrons$
- $ep \rightarrow Q + L \rightarrow hadrons + ...$
- $pp \rightarrow Z^{0'} \rightarrow hadrons$

Experimentally it is necessary to identify these heavy objects (e.g. by their invariant mass), determine their production mechanism (e.g. by their angular distribution), and obtain information about their couplings to quarks and leptons (e.g. by identifying the quarks into which they decay). This is the 'high Q^2'-problem addressed in the introduction: From the measurement of a jet we have to know the energy and direction as well as the flavour of the original parton.

5.1 Measuring the Energy and Direction of the Partons

Measurements at PETRA and PEP confirmed the expectation that the largest part of the energy is stored in charged particles, they add up to about 66 % [**3,31**] . About 27 % of the energy in a jet is carried by photons (mostly coming from π^0-decays) [**64,65**] . Neutrons and K_L^0's contribute about 6% to the energy (assuming the proton rates to be about equal to the neutron rates, and the K_S^0 - yield to be the same as the K_L^0 yield). A small amount of energy materialises in ν's and is therefore undetectable.

No sign of a dependence on the c.m. energy of the different contributions has been found, however they fluctuate strongly from event to event. Thus to obtain an appropriate measure of the jet energy and direction good calorimetry is essential: both for the electromagnetic and hadronic components of the events. Especially at eq and qq - colliders , where the partonic energy has to be inferred from the final products, calorimeters are the decisive part of the detector. E.g. for the ep-collider HERA, coming into operation at DESY in 1990, the importance of hadronic calorimetry for the determination of x and Q^2 has been stressed [**66**] . A detector without hadronic calorimetry, but which can measure the charged particle and electromagnetic component with high precision, would be plagued by large fluctuations in the neutral hadronic component. These would result in large fluctuations on the determination of the initial parton state. These fluctuations can be overcome by hadronic calorimetry.

At PETRA and PEP and presumably also at LEPI and SLC the e^+e^- - experiments however come along quite well without (hadronic) calorimetry. The basic advantage of

e^+e^- - collisions is the precise knowledge of the partonic c.m. system from the initial state: its total energy is determined by machine parameters and its uncertainty is $O(10^{-3})$, in addition the system is known to be at rest in the lab-system. These informations constrain the final state substantially. Using these constraints complete calorimetry does not seem to be essential, although it helps for some processes. This is especially true in the case where a single object is produced that decays into jets, e.g. $e^+e^- \rightarrow Z^0 \rightarrow q\bar{q}$.

Complete calorimetry becomes relevant, however, when two or more objects are produced that decay into several jets, e.g. $e^+e^- \rightarrow W^+W^-$, and the W's decay hadronically. Since jets are extended objects, particles from different jets can mix in direction and energy. An event e.g. of the type $e^+e^- \rightarrow W^+W^-$ (fig. 5.2.1a) which looks clear on the parton level (fig. 5.2.1.b), can exhibit a high confusion of particles from the various partons (5.2.1.c) after hadronisation. In addition, it should be kept in mind, that a quark in the decay $W \rightarrow q\bar{q}$ can radiate a gluon, i.e. in the example discussed, more jets have to be associated with a single W. Experimenters have to determine the properties of the particles from jets by associating them to one of the produced objects. However, due to the multitude of jets this association is ambiguous and the overall constraint in energy and momentum does not allow to fully constrain each of the objects individually. The case $e^+e^- \rightarrow W^+W^-$ will be discussed in more detail below.

The TASSO-collaboration [3] has measured how the energy in an e^+e^--event is distributed around the jet axis. For this analysis the event was divided into two hemispheres and the sum of momenta in each hemisphere was measured as a function of the angle α with respect to the jet axis . This result can be converted into the fraction of energy contained in a cone with half opening angle α around the jet axis. The outcome is displayed in fig. 5.2.2 for various c.m. energies [67] . This picture reveals that the energy has to be summed within a rather wide cone. A half opening angle of $\sim 40 - 50$ degrees is necessary even to collect only 90 % of the total energy. The dependence of the width of the energy-distribution on the total c.m. energy is seen to become rather weak at higher W's, a result supported by QCD Monte-Carlo calculations for the TeV-region at hadron colliders [68] . At high center of mass energies the large transverse component of the energy originates from hard gluon emission. The QCD matrix-element however varies only logarithmically with W and thus the W-dependence of the high transverse energy yield is small. Note that this energy distribution is averaged over all events. For each individual event the energy is not continously spread around the jet axis but e.g. concentrated in several more or less narrow cones. Still, the total energy of a primary parton can only be determined by summing the energy distribution within cones having substantial opening angles. Experimentally this can lead to considerable distortions when relevant distributions have to be determined using jets.

A case study has been made for the process $e^+e^- \rightarrow W^+W^-$, where both W's decay hadronically, assuming a c.m. energy of 200 GeV. Applying the second-order QCD-matrix element to the W decays this leads to a quite high number of jets. About 40% of all events have at least six jets. This leads to confusions which jet to associate to which W. Results of such an analysis are discussed in [69] . For the analysis detector effects have been

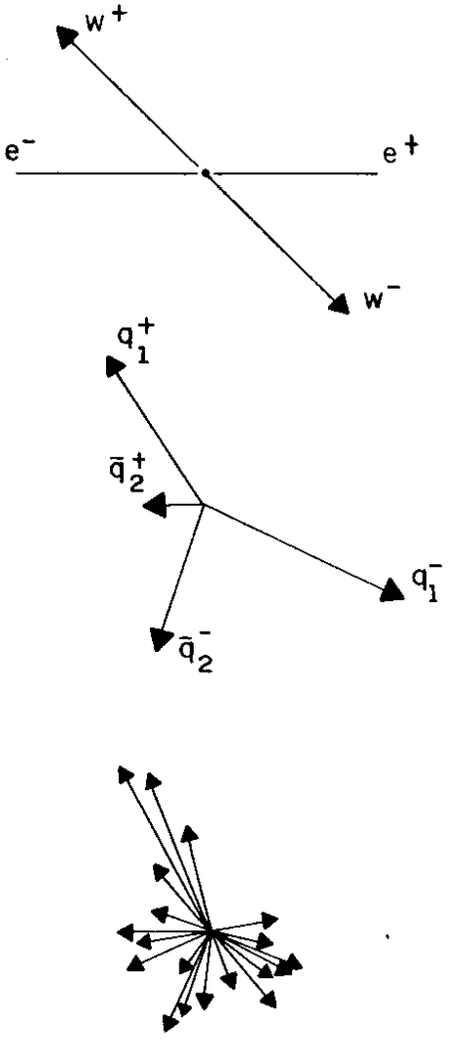

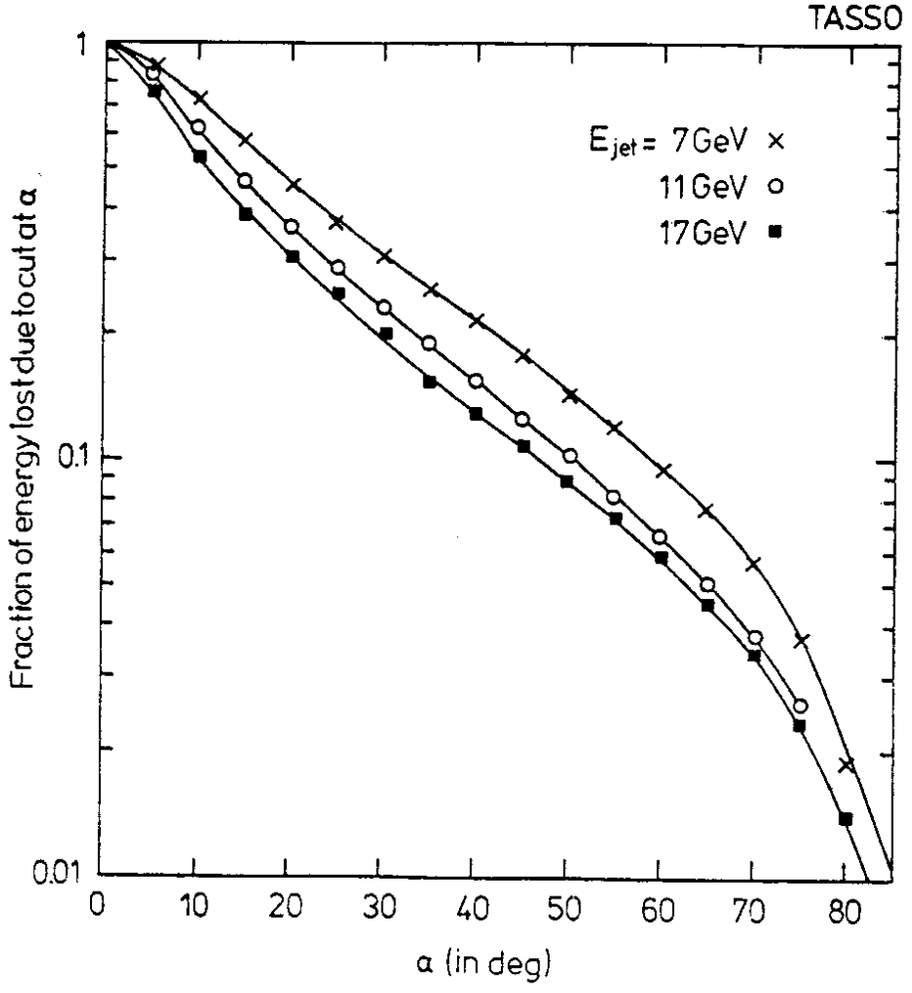

Fig. 5.2.2 Fraction of energy contained in a cone with half opening angle α around the jet axis measured at different jet energies. The lines are to guide the eye.

included by smearing the energy and direction of each parton by

$$\frac{\sigma(E)}{E} \quad \frac{\alpha}{\sqrt{E}} \quad , \quad \sigma(\theta) \quad 0.005\ rad$$

Here θ are the azimuthal and polar angles of the parton and α parametrises the quality of the energy resolution and is varied between 0 and 1 . From the smeared partons, jets were assigned to W's if the reconstructed masses of the two jet combinations were closest to the correct W-mass according to

$$d \quad min\,|\,(M_A - M_W)^2 + (M_B - M_W)^2|$$

This leads to a preferred association of partons to a W. The probability that this preferred assignement does not agree with the true assignment is displayed in fig. 5.2.3.

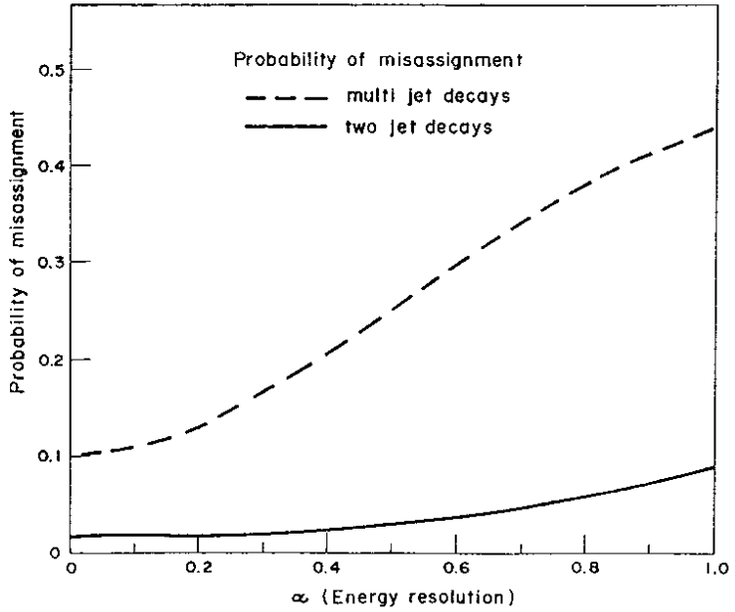

Fig. 5.2.3 Probability to misassign at least one jet to a W depending on the energy resolution $\frac{\sigma(E)}{E} = \frac{\alpha}{\sqrt{E}}$ of the detector. The probability is calculated with models that assume W-decays with and without QCD bremsstrahlung.

As can be seen the probability of confusion is strongly depending on the number of jets into which the W's will decay. It is a large simplification to assume just two-jet

decays of the W, and the confusion probability is considerable for the realistic assumption that gluon bremsstrahlung will occur in W-decays and an appropriate parametrisation of the detector. The broadness of jets leads to confusions in assigning partons or particles to some heavy object. It substantiates the comments about the growing importance of full calorimetry for e^+e^--detectors at energies where two heavy objects are produced that decay into jets. Nothing very specific about W-production entered the analysis. Thus its result is quite general : QCD bremsstrahlung in the decays of heavy objects complicate the experimental determination of their properties substantially.

5.2 Measuring the Charge of the Parton

An even more complicated problem is to translate the observable jet structure into information about the kind of original parton. As discussed before, the topological differences between the different flavours and gluons are small and it is difficult to exploit these differences to obtain a high efficiency with a good signal to background ratio. The prospects to identify them will be discussed in sections 5.3 and 5.4.

A less ambitious but often useful and important goal is to determine the sign of charge of the original parton, say into which hemisphere the negative quark is emitted . To obtain the charge direction, the results on long -range charge correlations, discussed in section 1.1, will be used. As was pointed out, the first quark is often found among the most energetic particles within a jet. This suggests proceeding in the following way (cp. [**8**]) :

- the event is divided into two hemispheres with respect to the eventaxis (e.g. using the sphericity algorithm).
- for each jet the jetcharge $Q_I = \sum q_i x_i^\alpha$ is calculated using the particles within a jet, $x_i = \frac{2p_i}{W}$ is the scaling variable and α is a parameter larger than 0 that has to be optimised. Simulation studies suggest $\alpha \sim 0.5$.
- The sign of the original parton in jet A is given by the sign of $Q_A - Q_B$.

The reliability

$$r = \frac{right\ prediction - false\ prediction}{all\ predictions}$$

of this method has to be found from Monte-Carlo simulations. As the distributions of weighted charges and their correlations in the data agree well with the model calculations, the results from the simulations should be reliable. From these one finds $r \sim 70 - 80\%$ depending on α and the detailed event selection applied.

It should be noted that r is flavour dependent. The reliabilities are different for charge $\frac{2}{3}$ and charge $\frac{1}{3}$ quarks as well as light and heavy quarks due to their different decay properties.

5.3 Measuring the Parton Flavour - c,b Tagging

As discussed above, the topological methods to tag flavours are not very promising at PETRA or PEP energies with the possible exception of the b quark. It can be anticipated that for $M_q << \sqrt{s}$ the topological differences between the bottom and lighter quarks become less significant. Consider e.g. the multiplicity for b-jets which is different to that found in u,d,s jets (cp. table 4) at $W = 29\ GeV$

$$\frac{n_{uds}}{n_b} = \frac{5.9}{7.9} = \frac{5.9}{2.4 + 5.5}$$

where the multiplicity of a b-jet is split into the contribution of the b-decay (~ 5.5) and the residual jet (~ 2.4). With increasing W this last contribution will increase in both types of jets similarly, whereas the b-decay multiplicity does not change, so that at higher W

$$\frac{n_{uds}}{n_b} = \frac{5.9 + \Delta}{(2.4 + \Delta) + 5.5} \longrightarrow 1 \quad for\ s \to \infty$$

Similar arguments apply for other varibles. E.g. the sphericity of two - jet bottom events will decrease rapidly, and larger sphericity values are dominated by QCD effects which are similar for both light and heavy quarks. Therefore topological methods to identify the jet flavour seem to have little promise.

Instead of using topological methods and to parametrise an event globally one has to consider the particle structure of an event. The highest momentum particle has to be identified and to be related to the original parton. This procedure was already quite successfully used for charm and bottom jets where the special properties of charm and bottom hadrons have been exploited. These fall into three categories

a. Mass reconstruction of c and b hadrons The charmed hadrons D^{**}, D^*, $D^{0,+,-}$, F, and Λ_c have been reconstructed within jets, the D^*giving an especially clean signal. Typically the detectable branching ratios of these decays are $\sim 3 - 4\%$ and require a good momentum resolution and in some cases an efficient π^0 detection. With this method however a good signal to background ratio has only been obtained for relatively high $x_c = \frac{2p_c}{W}$-values. It has been successfull because no other source of charmed particles (except from b-decays, which e.g. become more prominant at the Z^0) is relevant at PETRA and PEP energies . At higher c.m. energies, however, QCD effects will lower the x-values of charm production and in addition open phase space for charmed particles coming out of gluon jets. Still this mass reconstruction is presumably a very effective way to tag charmed jets. In the case of b-jets the reconstruction of the first produced hadron is less effective due to the high decay multiplicity. The two body decay branching ratios (like $B \to D^*\pi$, $D^*\rho^0$) are measured to be O(0.2%) [**70,71**] . Considering the detectable D^*branching ratios, experimental effects etc., the detection efficiency for exclusive b-decays is O($\sim 10^{-4}$)

such that even with the high rate of b events at the Z^0, only rather few B mesons will possibly be reconstructed .

b. High p_T leptons . Most information about b's within jets has up to now been obtained through the detection of high momentum, high p_T electrons and muons. Prompt leptons with these properties can only come from weakly decaying hadrons having a high mass. Therefore the signal to background ratio depends on the experimental ability to identify these prompt leptons. As discussed in section 4.1 the efficiencies to tag b quarks reached up to now are $\sim 2.5\%$ for a good signal to background ratio. Improvements on the lepton detection system may help to increase the efficiency. It will however be difficult to reach efficiencies beyond $\sim 10\%$ using both electrons and muons. Leptons with a high p_T can also come from c quarks, however as the charm mass is smaller than the bottom mass also the p_T of their leptonic decay products is smaller. Thus they are less easy to isolate.

c. Finite lifetime. One of the prime goals of the development of vertex detectors is to take advantage of the long lifetime of c and b mesons and tag them. Their lifetimes of $0.5 - 1/psec$ lead e.g. at the Z^0 to flightpaths of $\sim 2mm$ which are possible to detect in high resolution tracking devices. Although up to now no detector at an e^+e^- storage ring has successfully exploited the finite lifetime to tag flavours, optimistic estimates for new generation devices predict an efficiency of up to 40% to tag b events [**72**] . Again b-tagging is easier than c detection due to the additional constraints like high decay multiplicty and high masses . However combined with other criteria, the detection of a secondary vertex is a very promising tool also for charm jets.

process	s-quark ($s\bar{s}$, $u\bar{u}$)	u-quark ($u\bar{u}$, $s\bar{s}$)
prim.	0.18	0.14
second.	0.44	0.12
total	0.080	0.016

Table 5

5.4 Measuring the Parton Flavour - Light Quark Tagging

On the Z^0 it is even possible to obtain a sample of strange and up quarks with a good signal to background ratio. This result has been found by simulation studies for $Z^0 \rightarrow hadrons$ [**73**] . To be successfull a good K^+ and p - identification even at high momenta is assumed in accord with the design of several detectors for LEP or the SLC [**74,75,76,77**] . As discussed above, this does not help very much at PETRA and PEP energies , however on the Z^0 the production rates of primary s and u quark-types are about the same and repeating the calculation of table 3 on the Z^0 one finds a considerably improved signal to background ratio (table 5).

Thus, if the K^+ containing the primary quark can be found, the signal to background ratio is about 5 : 1 . In the method developed only K^+ with a $x > 0.6$ were used, similar to the selection of light quark samples by the HRS collaboration (see section 4.3) .

To suppress the high momentum K^+'s from the subsequent fragmentation the charge of the jet in the hemisphere opposite to the detected K^+

$$Q_{jet} = \sum q_i x_i^{0.5}$$

(see section 5.3) had to be negative, i.e. to have a sign opposite to the tagged particle. Folding in the experimental probability to find a K^+ (using the anticipated OPAL-$\frac{dE}{dx}$-measurement) the study suggests that about 3% of the strange events can be tagged. The signal to background ratio is $\sim$ 4 : 1.

The u-quark can be tagged in a similar way requiring a proton to be detected. The lower baryon yield decreases the efficiency to about 1%. No experimentally feasible way has been found to tag d-quarks (it would e.g. require neutron detection within a jet).

The exact values of the efficiencies using this method depends on the fragmentation functions which are only known indirectly. However many consistency checks are possible to estimate the validity of the simulations. For these results it is essential to assume that the development of a jet is independent of the original parton. The experimental evidence for this has been discussed in chapter 4 .

5.5 The Measurement of Partons - Conclusions

The experimental exploration of the standard model and even more the physics beyond it, will use quarks like the hadrons in past times. Instead of studying the decay $\rho^0 \to \pi^+\pi^-$, the decay $Z^0 \to q\bar{q}$ will be examined. This requires a detailed knowledge of how to obtain information about the original quark from the jet to be detected. Instead of hadron spectroscopy the energy regime $> 100\ GeV$ requires jet spectroscopy.

The determination of the energy and momentum is relatively straight forward using a calorimetric measurement. These experimental devices allow resolutions for single hadrons of

$$\sigma(E) \sim 0.35\sqrt{E} \quad and \quad \sigma(\theta) \sim 5mrad$$

In addition to these resolutions, however, distortions arising from the structure of jets have to be taken into account : jets are extended objects and the association of particles to jets is partly ambiguous. A case study related to this problem has been discussed for $e^+e^- \to W^+W^-$.

parton	method	efficiency ϵ	detector requirement
u	$p\bar{p}$ with x>0.6	1%	particle id.
d	?		
s	K^+K^- with x>0.6	3%	particle id.
c	mass reconst.	3%	momentum resolution
b	high p_T leptons secondary decay	$\leq$ 10% $\leq$ 40%	good μ, e id vertex detection
t	topology	dep. on M_t	particle rec.
g	?		

Table 6

The identification of the parton kind is a more difficult problem. Its prospects for LEP and SLC is summarised in table 6. As can be seen, the efficiencies for flavour tagging are rather low O(1-5 %), only the b-quark seems to be more easily detectable. Flavour tagging requires experimental devices to separate out special particles in a jet, like high momentum hadron identification, lepton identification and vertex detectors. This implies that the knowledge of the internal structure of jets is important also at very high energies.

6. Conclusions

A high fraction of publications from the experiments at PETRA and PEP contributed new information about the structure of jets. This considerable experimental progress in the recent years allows a detailed phenomenological insights into the jet development. Rather model independent properties have been studied, and the achievements in particle identification and correlation properties constrain the phenomenological description of fragmentation. A major progress has been reached in separating events originating from a known type of parton.

Together with general theoretical and phenomenological ideas these results are summarised in fragmentation models like the QCD shower model or more classical approaches like the string picture. Especially the QCD shower models have become more and more powerful and popular recently. The major step forward has been the theoretical prediction of coherent gluon radiation and the application of the models by experimenters to the measured energy and particle flow.

It is remarkable how well these models describe the data at a fixed energy. However, a well founded complete theoretical description of jet development is still lacking. In all these models the partons have to convert into hadrons, but the low Q^2 - region is not accessible to theoretical calculations yet. Still, the models developed for this transition seem to work. Open questions remain: e.g. it is not obvious, if the Q^2-dependence of the properties of hadronic events within these models is properly accounted for and no compelling way has been found to discriminate between the most successful models, the QCD shower algorithm and the string model. The probable increase in jet multiplicity at higher c.m. energies may indicate which way to proceed.

The insight into jets has developed quite far and we will be able to use jets as entities and manifestations of the more fundamental quarks and gluons. This aspect of jet physics will be of extreme relevance when exploring the energy regimes beyond the standard model - in not too far future.

Acknowledgements

This report grew out of numerous discussions with my colleagues at DESY, especially from the TASSO-collaboration. It is a pleasure to thank all of them for providing this cooperative and stimulating atmosphere.

I am grateful to M.Dittmar and P.Watson for many suggestions on this article. M.Ogg supplied useful informations from the CLEO-experiment. My special thanks go to Ken Bell whose thorough and critical comments helped to sharpen the text.

This report was presented during the $XXVI^{th}$ Cracow School of Theoretical Physics in Zakopane. I enjoyed the lively and critical discussions during this school in the beautiful surroundings of the Tatra mountains. For the invitation to this very effective and fruitful school I thank the organisers A.Bialas, K.Zalewski and W.Czech.

Last but not least go my thanks to A. Eskreys for his help, encouragement and profitable cooperation on some of the subjects presented.

References

[1] Review of Particle Properties. Phys.Lett. 170B (1986)

[2] G.Hanson et al.,Phys. Rev. Lett. 35(1977), 1609

[3] TASSO-collaboration, M.Althoff et al.,Z.Phys C22(1984),307

[4] TASSO-collaboration, R.Brandelik et al.,Phys. Lett. 114 B(1982),65

[5] PLUTO-collaboration, C.Berger et al.,Nucl. Phys B124(1983),189

[6] TASSO-collaboration, R.Brandelik et al.,Phys. Lett. 86 B(1979),243 , MARKJ - collaboration, D.P.Barber et al.,Phys. Rev. Lett. 43(1979),830 PLUTO-collaboration, C.Berger et al.,Phys. Lett. 86 B(1979),418, JADE-collaboration, W.Bartel et al., Phys. Lett. 91 B(1980), 142

[7] TASSO-collaboration, R.Brandelik et al.,Phys. Lett. 97 B(1980),453

[8] R.D.Field and R.P.Feynman Nucl. Phys B136(1978),1

[9] P.Hoyer et al.,Nucl. Phys B161(1979), 349

[10] B.Andersson et al., Phys.Rep. 97 (1983),33

[11] R.D.Field and S.Wolfram, Nucl. Phys B213(1983),65 ; T.D. Gottschalk, Caltech preprints CALT-68-946, CALT-68-1052

[12] G.Marchesini and B.R.Webber, Nucl. Phys B238(1984),1 ; B.R.Webber Nucl. Phys B238(1984),492

[13] T.F.Walsh and P.M.Zerwas, Phys. Lett. 44 B(1973), 195

[14] MAC-collaboration, E.Fernandez et al. Phys. Rev. Lett. 54(1985), 95

[15] S.Berends et al., Phys.Rev.D 31 (1985),2161

[16] S.Drell, D.Levy and T.M.Yan, Phys.Rev. 187(1969),2159

[17] TASSO-collaboration, R.Brandelik et al., Phys. Lett. 114 B(1982),65

[18] R.Baier and K.Fey, Z.Phys C2(1979), 239 ; G.Altarelli et al., Nucl. Phys B160(1979), 301

[19] TASSO-collaboration, M.Althoff et al., Phys. Lett. 135 B(1984),243

[20] TASSO-collaboration, M.Althoff et al., Phys. Lett. 139 B(1984),126

[21] TASSO-collaboration, M.Althoff et al., Z.Phys C17(1983),5

[22] H.Aihara et al., Phys. Rev. Lett. 54(1985),274

[23] C.de la Vaissierre et al., Phys. Rev. Lett. 54(1985),2071

[24] TASSO-collaboration, M.Althoff et al.,Z.Phys C27(1985),27

[25] B.Andersson et al., Phys. Lett. 94B B(1980), 211

[26] JADE-collaboration, W.Bartel et al.,Phys. Lett. 101 B(1981),129 ; Phys. Lett. 134 B(1984),275

[27] H.Aihara et al., Phys. Rev. Lett. 54(1985),270 ; Z.Phys C28(1985),31

[28] TASSO-collaboration, M.Althoff et al.,Z.Phys C29(1985),29

[29] B.I.Ermolaev and V.S.Fadin, JETP Lett. 33 (1981),269 ; Yu.L.Dokshitzer, V.S.Fadin and V.A.Khoze ,Phys. Lett. 115 B(1982),242, Z.Phys C15(1982),325 ; Z.Phys C18(1983),37

[30] A.H.Mueller , Phys. Lett. 104 B(1981),161 ; A.Bassetto et al., Nucl. Phys B207(1982),189

[31] D.Bender et al. Phys. Rev.D31 (1985),1

[32] H.Aihara et al., Phys. Rev. Lett. 52(1984),577

[33] Ya.I.Azimov et al. Z.Phys C31(1986),213

[34] S.Wolfram in Proc. 15^{th} Rencontre de Moriond (1980), ed. J. Tran Thanh Van

[35] D.Amati and G.Veneziano, Phys. Lett. 83 B(1979),87

[36] JADE-collaboration, W.Bartel et al.,Phys. Lett. 157 B(1985), 340

[37] Ya.I.Azimov et al., Leningrad preprint (1985),1051

[38] D.Saxon in Proc. of the EPS conference on High Energy Physics, Bari, Italy $18^{th} - 24^{th}$ July,1985

[39] ARGUS-collaboration, to be published

[40] TASSO-collaboration, M.Althoff et al.ZFP 26 (1984), 181

[41] TASSO-collaboration, M.Althoff et al., Phys. Lett. 130 B(1983),340

[42] V.Cerny, P.Lichard and J.Pisut, Phys. Rev D16 (1977),2822 ; Acta Phys. Polonica B10 (1979),629 ; Pys. Rev. D18 (1978),2409 ; Czech J. Phys. B31 (1981),1302

[43] T.Meyer, Z.Phys C12(1982),77

[44] B.Andersson et al., Nucl. Phys B197(1982),45

[45] M.G.Bowler, Oxford Nuclear Physics Report 76/81 (1981)

[46] T. de Grand, Phys. Rev. D26 (1982),3298

[47] T.Bowcock et al., Phys. Rev. Lett. 55(1985), 923

[48] C.Peterson et al., Phys.Rev. D27, (1983), 105

[49] T.Sjøestrand in Proc. of the $XXIII^{rd}$ International Conference on High Energy Physics, Berkeley, California 1986, to be published

[50] M.Sakuda et al., Phys. Lett. 152 B(1985), 399

[51] S.Bethke, Z.Phys C29(1985), 175

[52] R.Giles et al., Phys. Rev. D30 (1984), 2279

[53] TASSO-collaboration, M.Althoff et al., Phys. Lett. 149 B(1984),524

[54] TASSO-collaboration, M.Althoff et al., Phys. Lett. 138 B(1984),317

[55] P.Kesten et al., Phys. Lett. 161 B(1985), 412

[56] JADE-collaboration, W.Bartel et al.Phys. Lett. 130 B(1983), 454

[57] A.Petersen et al. , Phys. Rev. Lett. 55(1985), 1954

[58] M.Derrick et al., Phys. Lett. 165 B(1985), 449

[59] UA1-collaboration, G.Arnison et al., CERN-EP/86-55

[60] A.Ali et al., Phys. Lett. 93 B(1980), 155

[61] R.Schindler et al., Phys. Rev. D 24 (1981), 78

[62] A.H.Mueller Nucl. Phys B241(1984), 141

[63] TASSO-collaboration, M.Althoff et al., Phys. Lett. 138 B(1984),441

[64] JADE-collaboration, W.Bartel et al.Z.Phys C9(1981), 315

[65] CELLO - collaboration, H.J.Behrend et al., Z.Phys C14(1984), 189

[66] M.Holder in Proceedings of the Workshop Experimentation at HERA, NIKHEF Amsterdam, June 9-11, 1983

[67] P. Mättig, TASSO-note 305, unpublished

[68] T.Åkesson et al., in Large Hadron Collider in the LEP Tunnel Vol. I, Proceedings of the ECFA-CERN Workshop held at Lausanne and Geneva 21-27 March 1984 ed. M.Jacob ECFA 84/85 and CERN 84-10

[69] P.Mättig, Contribution to the working groups preparing the Workshop on LEP2 at Aachen, 29.9.-1.10.1986 and to be published

[70] Branching ratios 2-body B-dec CLEO

[71] ARGUS-collaboration, H.Albrecht et al., DESY 86-074

[72] A.Breakstone et al., Proposal for the Addition of a Silicon μ-strip Detector to the Mark II Detector at the SLC, July 1985 and private communication A.Schwarz

[73] M.Dittmar, Internal OPAL note and private communication

[74] OPAL-collaboration, Technical proposal CERN/LEPC/83-4,LEPC/P3

[75] H.M.Fischer et al., CERN-EP/86-59

[76] DELPHI-collaboration, Technical proposal

[77] SLD-collaboration, Technical proposal